

SYSTEM IDENTIFICATION OF GENERAL AVIATION AIRCRAFT
USING THE FILTER ERROR TECHNIQUE

Except where reference is made to the work of others, the work described in this thesis is my own or was done in collaboration with my advisory committee. This thesis does not include proprietary or classified information.

Dakshesh Patel

Certificate of Approval:

John E. Cochran, Jr.
Professor
Aerospace Engineering

Gilbert L. Crouse, Chair
Associate Professor
Aerospace Engineering

David A. C Ricci
Professor
Aerospace Engineering

Joe F. Pittman
Interim Dean
Graduate School

SYSTEM IDENTIFICATION OF GENERAL AVIATION AIRCRAFT
USING THE FILTER ERROR TECHNIQUE

Dakshesh Patel

A Thesis

Submitted to

the Graduate Faculty of

Auburn University

in Partial Fulfillment of the

Requirements for the

Degree of

Master of Science

Auburn, Alabama
December 17, 2007

SYSTEM IDENTIFICATION OF GENERAL AVIATION AIRCRAFT
USING THE FILTER ERROR TECHNIQUE

Dakshesh Patel

Permission is granted to Auburn University to make copies of this thesis at its discretion, upon the request of individuals or institutions and at their expense. The author reserves all publication rights.

Signature of Author

Date of Graduation

VITA

Dakshesh Patel was born to Mahesh and Geeta, on March 15, 1983 in Ahmedabad. He attended Nirma Institute of Technology, Ahmedabad and graduated in July 2004 with Bachelor of Engineering in Instrumentation and Control. He joined Aerospace Engineering Program at Auburn University as a Masters student in August 2004.

THESIS ABSTRACT

SYSTEM IDENTIFICATION OF GENERAL AVIATION AIRCRAFT

USING THE FILTER ERROR TECHNIQUE

Dakshesh Patel

Master of Science, December 17, 2007
(B.E., Nirma Institute of Technology, Gujarat University, 2004)

123 Typed Pages

Directed by Gilbert L. Crouse

An overview of some past and modern applications of system identification techniques to aircraft is presented in this thesis, which traces progress and accomplishments in the field of system identification - especially application to aircraft. The thesis also includes the definition, meaning, importance, applications and necessity of the same. The fundamental parts of system identification, including model postulation, experimental design, data analysis, parameter estimation, and model validation are explained. The filter error technique of data analysis is detailed, for both linear and nonlinear systems. Techniques to predict aircraft stability and control derivatives theoretically and analytically are explained in some details. Two successfully investigated experiments of system identification using flight data with results and comparison of the estimated parameters with published data are demonstrated with details. The thesis is completed by some remarks made on possible future advancement and concluding notes.

ACKNOWLEDGMENTS

The author would like to thank his research advisor, Dr. Gilbert L. Crouse, for rendering constant guidance and motivation throughout his research. He also thanks Dr. Crouse for showing complete trust in his abilities and providing him with an opportunity to conduct research in the exciting field of system identification. Dr. Crouse is a great mentor and working with him was a wonderful and memorable experience for Dakshesh. The author would like to express his gratitude to Dr. John E. Cochran for teaching the courses which greatly helped him in understanding the research problem and also for being part of his graduate committee. He would like to thank Dr. David A. Cicci, for teaching the fundamentals of estimation theory through orbit determination class and also for serving as a graduate committee member.

The author is thankful to Ran Dai and Daroe Lee, for their friendship and help in understanding the dynamics and control subjects. He would like to acknowledge his friends at Auburn, with whom he spent memorable years. Particularly Palak, Vinita and Dhrumil's support and encouragement have always made his stay at Auburn, pleasant and enthusiastic.

The author wishes to dedicate this work to his parents and teachers for their enduring love, immense moral support and encouragement in the journey of life.

Style manual or journal used AIAA Journal of Aircraft

Computer software used LATEX and the departmental style-file "aums.sty"

TABLE OF CONTENTS

LIST OF FIGURES	x
LIST OF TABLES	xii
NOMENCLATURE	xiii
1 INTRODUCTION	1
1.1 System Identification - A Definition	1
1.1.1 Significance and Necessity of System Identification	2
1.1.2 Objectives of Research	4
1.2 Problem Description	5
1.3 Progress of Aircraft System identification	7
1.3.1 System Identification in General	7
1.3.2 System Identification of Aircraft	8
1.3.3 Deterministic and Non-Deterministic Analysis	10
1.3.4 Latest Techniques of System Identification	13
2 BACKGROUND AND THEORETICAL DEVELOPMENT	16
2.1 Dynamical Model Description	16
2.2 Cost Function (Performance Index) J	17
2.3 Essentials of Cost Function Minimization	17
2.4 Modified Newton-Raphson Algorithm	20
3 SYSTEM IDENTIFICATION OF GENERAL AVIATION AIRCRAFT	23
3.1 Filter Error Technique for Linear Systems	23
3.1.1 Kalman Filter	25
3.1.2 Solution of Riccati Equation	26
3.1.3 Formulations for Process Noise	28
3.1.4 The Filter Error Algorithm for Linear Systems	30
3.1.5 Parameter Update	32
3.2 Filter Error Technique for Non-linear Systems	36
3.2.1 Steady State Filter	38
3.2.2 Parameter Update	41

4	PREDICTION OF AIRCRAFT STABILITY AND CONTROL DERIVATIVES	42
4.1	Steady State Coefficients	43
4.2	Stability Derivatives	45
4.2.1	Aircraft Speed Derivatives	46
4.2.2	Angle of Attack Derivatives	47
4.2.3	Angle of Sideslip Derivatives	48
4.2.4	Roll Rate Derivatives	51
4.2.5	Pitch Rate Derivatives	53
4.2.6	Yaw Rate Derivatives	53
4.3	Control Derivatives	55
4.3.1	Aileron Control Derivatives	56
4.3.2	Elevator Control Derivatives	57
4.3.3	Rudder Control Derivatives	57
5	INVESTIGATED EXAMPLES OF SYSTEM IDENTIFICATION USING FLIGHT TEST DATA	59
5.1	Estimation of Lateral Motion Derivatives using the Simulated Flight Data .	59
5.1.1	Comparison of the Results with the Original Experiment	61
5.1.2	Responses and Results	63
5.2	Estimation of Longitudinal Motion Derivatives of HFB-320 Aircraft	67
5.2.1	Comparison of the Results with the Original Experiment	70
5.2.2	Responses and Results	70
5.3	System Identification Applied to Model Aircraft Trainer	73
5.3.1	The Investigated Aircraft Trainer - Hanger 9 Extra Easy	73
5.3.2	Responses and Results	74
5.4	Model Validation	87
6	SUMMARY	88
6.1	Concluding Notes	88
6.2	Expected Future Applications of System Identification to Aircraft	89
	BIBLIOGRAPHY	91
A	DISCRETIZATION OF CONTINUOUS-TIME STATE EQUATION	99
A.1	Need of Discretization	99
A.2	Determine Θ and Λ	100
B	NUMERICAL INTEGRATION USING RUNGE-KUTTA METHOD, ORDER 4	102

LIST OF FIGURES

1.1	Block Diagram for System Identification to aircraft [1]	14
3.1	Block Diagram for Filter Error Technique [68]	24
3.2	Algorithm of Filter Error Technique for Linear Systems [1]	31
3.3	Algorithm of Filter Error Technique for Nonlinear Systems [1]	37
4.1	Determination of Drag Coefficient from a known Lift Coefficient	44
5.1	The DLR <i>de Havilland DHC – II</i> Research Aircraft [84]	60
5.2	Comparison of Estimated(green) and Measured(blue) Responses for the Lateral Directional Motion of Aircraft	64
5.3	Convergence Plots of Dimensional Derivatives for Lateral Directional Motion of Aircraft	65
5.4	Cost Function Reduction for Lateral Directional Motion of Aircraft	66
5.5	The DLR <i>HFB – 320</i> Research Aircraft [87]	67
5.6	Comparison of Estimated(green) and Measured(blue) Responses for the Longitudinal Directional Motion of Aircraft	71
5.7	Convergence Plots of Non-Dimensional Derivatives for Longitudinal Directional Motion of Aircraft	72
5.8	Inputs for Longitudinal Motion	72
5.9	Cost Function Reduction for Longitudinal Motion	73
5.10	Aircraft Trainer - Hanger 9 Extra Easy [91]	74
5.11	Comparison of Estimated(green) and Measured(blue) Responses for the Lateral Directional Motion of Aircraft	77

5.12	Convergence Plots of Dimensional Derivatives for Lateral Directional Motion of Aircraft	78
5.13	Cost Function Reduction for Lateral Directional Motion of Aircraft	79
5.14	Comparison of Estimated(green) and Measured(blue) Responses for the Lateral Directional Motion of Aircraft	80
5.15	Convergence Plots of Dimensional Derivatives for Lateral Directional Motion of Aircraft	81
5.16	Cost Function Reduction for Lateral Directional Motion of Aircraft	82
5.17	Comparison of Estimated(green) and Measured(blue) Responses for the Longitudinal Directional Motion of Aircraft	84
5.18	Convergence Plots of Non-Dimensional Derivatives for Longitudinal Directional Motion of Aircraft	85
5.19	Input for Longitudinal Motion	86
5.20	Cost Function Reduction for Longitudinal Motion	86

LIST OF TABLES

5.1	Estimated dimensional derivatives of lateral motion of aircraft	62
5.2	Estimated non-dimensional derivatives of longitudinal motion of aircraft . .	69
5.3	Aerodynamic, geometric and mass data for the aircraft trainer	75
5.4	Comparison between the predicted values and the estimated values of the dimensional derivatives for the lateral motion of the aircraft trainer	76
5.5	Comparison between the predicted values and the estimated values of the dimensional derivatives for the lateral motion of the aircraft trainer	82
5.6	Comparison between the predicted values and the estimated values of the non-dimensional derivatives for the longitudinal motion of aircraft trainer .	83

NOMENCLATURE

1. English Symbols

$a.c.$	aerodynamic center
A	state matrix of a linear system, size $n \times n$
$A_h = b_h^2 / S_h$	horizontal tail aspect ratio
$A_v = b_v^2 / S_v$	vertical tail aspect ratio
$A_w = b^2 / S$	wing aspect ratio
a_x, a_y, a_z	accelerations along x, y, z body axes, ft/s^2
b	wing span
b_h	horizontal tail span
b_v	vertical tail span
b_x, b_y	bias parameters of state and observation equations
c	chord, ft
\bar{c}	mean geometric chord, ft
c_r	root chord, ft
c_t	tip chord, ft
$c.g.$	aircraft center of gravity
C	observation matrix, size $m \times n$
C_D	aircraft drag coefficient
C_{D_0}	zero-lift drag coefficient

C_l	aerodynamic rolling moment coefficient
C_L	aircraft lift coefficient
C_{L_0}	lift coefficient at zero angle of attack
C_m	aerodynamic pitching moment coefficient
C_n	aerodynamic yawing moment coefficient
C_X	coefficient of longitudinal force
C_Y	coefficient of lateral(side) force
C_Z	coefficient of vertical force
D	Drag
e	span efficiency factor
e^j	j^{th} unit vector
F	state noise matrix, size $n \times n$ also: aerodynamic force, N
F_G	magnitude of force due to gravity, N
F_T	magnitude of force due to thrust, N
F_e	net thrust magnitude, N
$f[\cdot]$	vector of system state functions
G	measurement noise matrix, size $m \times m$ also: moment, Nm
g	acceleration due to gravity, ft/s^2
$g[\cdot]$	system observation function

I	inertia matrix
I_{xx}	rolling moment of inertia in body axes, $slug-ft^2$
I_{xz}	XZ product of inertia in body axes, $slug-ft^2$
I_{yy}	pitching moment of inertia in body axes, $slug-ft^2$
I_{zz}	yawing moment of inertia in body axes, $slug-ft^2$
J	cost function
K	filter-gain matrix, size $n \times m$
k	discrete-time index
l_f	fuselage length
l_p	horizontal distance between vertical tail a.c. and aircraft wing a.c.
l_v	horizontal distance between vertical tail a.c. and aircraft c.g.
L	lift
m	aircraft mass, lb also: number of observation variables
$m.g.c.$	mean geometric chord, ft
M	free stream mach number
N	number of data points
n	number of state variables
P	covariance matrix of the state error, size $n \times n$
p, q, r	roll, pitch, and yaw rates, rad/s
$\dot{p}, \dot{q}, \dot{r}$	roll, pitch, and yaw accelerations, rad/s^2

\bar{q}	dynamic pressure, N/ft^2
r_k	k^{th} diagonal element of R
R	covariance matrix of residuals (innovations), size $m \times m$
R_N	reynold's number
S	wing area, ft^2
$S_{b_{fuse}}$	fuselage base area, ft^2
S_{fuse}	maximum fuselage cross section area, ft^2
S_h	horizontal tail area, ft^2
S_{plf}	aircraft planform area, ft^2
S_v	vertical tail area, ft^2
S_{wet}	total wetted area of aircraft, ft^2
s	number of input variables
t	time, s
t/c	thickness ratio at \bar{c}
u	control input vector, size $s \times 1$
u, v, w	velocity components along x, y, and z body axes, ft/s
v	measurement noise vector, size $m \times 1$
V	airspeed, ft/s
\bar{V}_h	horizontal tail volume coefficient
w	state noise vector, size $n \times 1$
W	aircraft weight, lb

x	state vector, size $n \times 1$
X_{ac}	longitudinal position of a.c. on wing m.g.c., ft
X_{ac_h}	longitudinal position of horizontal tail a.c. on wing m.g.c., ft
X_w	longitudinal distance from wing quarter chord m.g.c. to c.g., ft
y	observation vector, size $m \times 1$
z	measurement vector, size $m \times 1$
z_f	vertical height of fuselage at wing root chord, ft
z_p	vertical distance between vertical tail a.c. and aircraft wing a.c., ft
z_v	vertical distance between vertical tail a.c. and aircraft c.g., ft
z_w	wing distance to fuselage centerline, ft

2. Stability and Control Derivatives

C_{D_V}	non-dimensional derivative of drag with respect to speed
C_{L_V}	non-dimensional derivative of lift with respect to speed
C_{m_V}	non-dimensional derivative of pitching moment with respect to speed
C_{D_α}	non-dimensional derivative of drag with respect to angle of attack
C_{L_α}	non-dimensional derivative of lift with respect to angle of attack
C_{m_α}	non-dimensional derivative of pitching moment with respect to angle of attack
C_{m_q}	derivative of pitching moment with respect to pitch rate
$C_{m_{\delta_e}}$	derivative of pitching moment with respect to elevator deflection
L_p	derivative of rolling moment with respect to roll rate

L_r	derivative of rolling moment with respect to yaw rate
L_{δ_a}	derivative of rolling moment with respect to aileron deflection
L_{δ_r}	derivative of rolling moment with respect to rudder deflection
L_v	derivative of rolling moment with respect to lateral(side) velocity
L_β	derivative of rolling moment with respect to sideslip angle
N_p	derivative of yawing moment with respect to roll rate
N_r	derivative of yawing moment with respect to yaw rate
N_{δ_a}	derivative of yawing moment with respect to aileron deflection
N_{δ_r}	derivative of yawing moment with respect to rudder deflection
N_v	derivative of yawing moment with respect to lateral(side) velocity
N_β	derivative of yawing moment with respect to sideslip angle
Y_p	derivative of side-force with respect to roll rate
Y_r	derivative of side-force with respect to yaw rate
Y_{δ_a}	derivative of side-force with respect to aileron deflection
Y_{δ_r}	derivative of side-force with respect to rudder deflection
Y_v	derivative of side-force with respect to lateral(side) velocity
Y_β	derivative of side-force with respect to sideslip angle

3. Greek Symbols

α	angle of attack, <i>deg</i>
β	sideslip angle, <i>deg</i>

	also: $(1 - M^2)^{1/2}$
γ	flight path angle, <i>deg</i>
Γ	dihedral, <i>deg</i>
$\delta_a, \delta_e, \delta_r$	aileron, elevator, and rudder deflections, <i>deg</i>
δx	perturbation in x
$\delta\Theta$	perturbation in Θ
Δt	sampling time, <i>s</i>
$\Delta\Theta$	vector of parameter update
ϵ	downwash angle at the horizontal tail, <i>deg</i>
ϵ_t	wing twist angle, <i>deg</i>
η	span fraction
η_h	ratio of horizontal tail to wing dynamic pressure
$\lambda = c_t/c_r$	taper ratio
$\Lambda_{c/2}$	semi-chord sweep angle, <i>deg</i>
$\Lambda_{c/4}$	quarter-chord sweep angle, <i>deg</i>
Λ_{LE}	leading edge sweep angle, <i>deg</i>
μ	coefficient of viscosity for air
ω	angular velocity, <i>rad/s</i>
Φ	vector of unknown parameters
ρ	density of air, <i>lb/ft³</i>
σ	side-wash angle, <i>deg</i>

σ_T	tilt angle of the engines, <i>deg</i>
θ	pitch angle, <i>deg</i>
Θ	state transition matrix
ϑ	vector of process noise distribution matrix, F
ζ	vector of system parameters

4. Superscripts

T	transpose
-1	inverse
\sim	predicted estimates
\wedge	corrected estimates

5. Subscripts

a	aileron
b	base
cg	center of gravity
cs	cross sectional
e	elevator
fus	fuselage
h	horizontal tail
i, j	general indices

k	discrete-time index
LE	leading edge
m	measured variables
max	maximum
M	(at a given) mach number
p	perturbed variables
plf	planform
r	rudder
ref	reference, usually the wing, or a point on the wing
v	vertical tail
w	wing
wet	wetted
0	initial condition

CHAPTER 1

INTRODUCTION

The thesis describes the system identification technique and its applications related only to aircraft, but the system identification has been successfully applied to many diverse fields. The system identification is basically related to modeling from experimental data and can be applied to many different fields such as: economics, biology, materials, engineering, automobiles, medicine and aerospace engineering.

1.1 System Identification - A Definition

System identification is a discipline of science which attempts to answer the inverse problem. It tries to characterize a system in a suitable form based on observations of the system's behavior. The process of system identification involves certain fundamental assumptions [1]:

1. The true state of the dynamic system is deterministic.
2. Physical principles underlying the dynamic process can be modeled.
3. It is possible to carry out specific experiments.
4. Measurements of system inputs and outputs are available.

In the year 1962, Zadeh [2] gave a technical definition for system identification as: "System identification is the determination, on the basis of observation of input and output, of a

system within a specified class of systems to which the system under test is equivalent.” Several important features of system identification are highlighted by this description: the necessity of obtaining input and output data, model characterization and selecting the best model from the selected class. Iliff [3] provided a philosophical definition in contrast with the above technical definition as: “Given the answer, what are the questions, that is, look at the results and try to figure out what situation caused those results.” This definition points out the prime approach behind the model building process, namely that system identification is an inverse problem.

1.1.1 Significance and Necessity of System Identification

The system identification tries to determine the best parameters for an assumed mathematical model, which is made up of differential equations. The unknown parameters are determined indirectly from measured data. Considering the aircraft system identification problem, assume Φ is an unknown parameter vector, which contains unknown stability and control parameters of the dynamics equations, which are to be estimated. As a first part of system identification, a parameter estimation technique is used to estimate the unknown parameter vector Φ , such that the system response y fits the measured system response z adequately. In aircraft system identification the measured system response is typically flight test data. After the parameter estimation is performed, a second and more important part, known as model validation needs to follow. It evaluates model reliability. If it seems that the identified model does not agree with the specific system standards and also the

statistical properties of the estimated parameters do not agree with the standards, then the postulated model structure needs to be changed. Generally both steps must be repeated again and again until the model is validated.

If the experimental model is already validated, then only the first part, parameter estimation, is dealt with. If the model structure is not known and adequate information about the system structure is not available, the system identification technique is dealt with as a whole, which includes both parameter estimation and model validation.

After mentioning the definition, meaning and significance of system identification and parameter estimation, the next question is, what is the necessity of system identification. Why and where is system identification needed? This question must be answered due to the two following examples of questions that have been raised about the utility of system identification.

1. During one of the early American Institute of Aeronautics and Astronautics (AIAA) conferences, someone raised a question: “When the aircraft is past the design and production stage, and already flying, why and where do you need system identification?” [4]
2. An anonymous paper reviewers comment: “After perhaps 30 years of journal articles and conferences on system identification, hardly any results have been of engineering utility. Or if they are in use, the fact is not widely published.” [4]

In flight vehicle development, system identification is a necessary step because it leads to adequately accurate and validated mathematical models of flight vehicles, which are required to [1],

1. understand the cause-effect relationship that underlines a physical phenomenon,
2. investigate system performance and characteristics,
3. verify wind-tunnel and analytical predictions,
4. develop high-fidelity aerodynamic databases for flight simulators meeting FAA fidelity requirements,
5. support flight envelope expansion during prototype testing,
6. derive high-fidelity and high-bandwidth models for in-flight simulators,
7. design flight control laws including stability augmentation systems,
8. reconstruct the flight path trajectory, including wind estimation and incidence analysis,
9. perform fault-diagnosis and adaptive control or reconfiguration, and
10. analyze handling qualities specification compliance.

Due to the advantages and the uses given above the system identification is made an essential part of aerospace system design and development.

1.1.2 Objectives of Research

The aim of this thesis and research work, is to contribute to the field of system identification of aircraft which has advanced over the recent decades, concentrating specifically

on nonlinear systems and time domain methodologies. Efficient and effective system identification of aircraft is only possible if the applied approach is well coordinated and follows specific research guidelines. The thesis uses the filter error approach for all three examples and tries to accommodate full details of such an efficient approach, summarizing the general important concepts, techniques, computational procedures and three selected examples, which were investigated based on the method.

1.2 Problem Description

The objective of system identification is to estimate the values of some unknown parameters in the system equations, which best represent the actual aircraft response, given a set of flight time histories of an aircraft's response variables. Here, the unknown parameters are stability and control parameters.

The typical mathematical approach to this problem is to minimize the difference between the flight response and the response computed from the system equations. This difference can be defined for each response variable as the integral of the error squared. Then the signal errors can be multiplied by weighting factors and summed to obtain the response error which defines an integral squared error criterion.

A mathematically more precise formulation can be made in probabilistic terms. A probability that the estimated aircraft response time histories take on the values actually observed can be defined for each possible estimate of unknown parameters. These parameter

estimates should be chosen so that this probability is maximized. This is known as a maximum likelihood formulation of the problem.

To describe the maximum likelihood estimator mathematically, it is necessary to define the equations of motion for the aircraft system. The following steps should be followed.

1. Derive the dynamical equations of motion.
2. Predict the unknown stability and control parameters.
3. Define the control inputs.
4. Express integral squared error criterion (to find a vector of unknowns), which minimizes the cost function (performance index) J .
5. Estimate the state error covariance matrix to construct the likelihood function.
6. Minimize the cost function. The modified Newton-Raphson method seems most suitable for aircraft derivative determination, both in terms of computer time and convergence properties.
7. Include prior information. Information from wind tunnel tests, previous real-time flight tests and simulated flight test results are often available with the values of some of the aircraft derivatives. It may be desirable to include this information in the algorithm. The use of this information is particularly important when there is a linear dependence between the response and the unknown parameters.

1.3 Progress of Aircraft System identification

A brief survey of the various contributions to the system identification field is presented in this section, starting with applications in many fields. Applications to aircraft will follow. Finally, the most modern techniques are briefed.

1.3.1 System Identification in General

The evolution from older system identification methods to statistically more accurate approaches has been gradual. References can be found going back to the 18th century, when Gauss [5] and Bernoulli [6] approached the system identification problem. The oldest reference was found in the year 1777, when Bernoulli arrived at a solution by differentiating the likelihood function [6]. Bernoulli used the concepts of maximum likelihood and least-squares solution, though he did not introduce these terms. In the year 1809, Gauss [5] used the maximum likelihood principle. In the reference mentioned, he discussed the least-squares method for orbit determination of the earth from astronomical measurements.

Following the fundamental methods of Bernoulli and Gauss during the 18th century, the maximum likelihood estimator was first discussed by Fisher [7] in the year 1912, as a general statistical parameter estimator. Douglas [8] discussed “Inverse Problem Theorems” in 1940. Feldbaum [9] considered the identification and control of the system as a single problem in the “dual-control” theory; which was a little different than others, but still his work was one of the most significant and also aimed at the present direction of investigation.

Research work in system identification theory prior to 1970, has been briefed in outstanding research survey papers [10-13].

There are two kinds of system identification problems: deterministic (without state noise) and non-deterministic (with state noise). Until the early forties, work on system identification focus on the deterministic problem. But, succeeding the initial work in 1941-1942 of Kolmogorov [14] and Wiener [15] the focus gradually shifted from deterministic estimation to stochastic estimation. It was in the year 1960, when Kalman [16] followed basic theories of Wiener and formulated a recursive solution to a filtering problem. This recursive solution was directly executable through digital computations. Therefore, the Kalman filter became popular quickly. Today it is the most widely used method for stochastic estimation. The first experimentation of the maximum likelihood estimator on a digital computer and application to parameters estimation in an industrial plant was done by Astrom and Bohlin in 1965 [17]. This was the beginning of the modern era of system identification methods.

1.3.2 System Identification of Aircraft

The aerodynamic modeling, which obtains relationships between the three forces X, Y and Z along the three cartesian coordinates, and the moments L, M and N about these axes as functions of linear translational motion variables u, v, w and rotational rates p, q, r was introduced in the early 20th century [18, 19]. This was the initiation of the evolution of aircraft system identification. After the pioneering work of Bryan [18], numerical, statistical and experimental research was started in the field of real-time dynamics stability

and control. Glauert [20] initiated analyzing the phugoid motion of an aircraft in 1919 and Norton [21, 22] presented papers in 1923 on estimation of stability and control derivatives. The developments over the last nine decades have led to three different, but complementary techniques for determining aerodynamic coefficients: 1) analytical methods, 2) wind-tunnel methods, and 3) flight test methods [19].

The analytical methods and the wind-tunnel methods are performed to generate basic information about the aerodynamic flight coefficients. Research in the computational fluid dynamics field in recent years has positively affected the analytical approaches by providing numerical solutions of complete configurations via sophisticated and advanced Euler and Navier-Stokes flow solvers [19, 23, 24]. Experimental methods are important to validate the analytical estimations. Wind-tunnel techniques, have in the past provided a huge amount of data on innumerable flight vehicle configurations and are, as a rule, a basis for any new flight vehicle design [19]. These techniques are, however, often associated with certain limitations of validity arising out of, for example, model scaling, Reynolds number, dynamic derivatives, cross coupling, and aero servo elasticity effects [19]. Determination of aerodynamic derivatives from flight measurements is, therefore, important and necessary to reduce limitations and uncertainties of the aforementioned two methods [19] and [25].

While detailing the chronological survey of research which led to the development and universal acceptance of the maximum-likelihood estimation technique for aircraft stability and control derivatives estimation, the more straightforward deterministic analysis will be discussed first, which will be followed by non-deterministic analysis. References [26] and [27]

discuss some of the investigations in estimation of unknown stability and control derivatives of an aircraft from aircraft dynamic response data.

1.3.3 Deterministic and Non-Deterministic Analysis

1. **Deterministic Analysis:** System identification methods have become more elegant and complex since Kalman's contribution. The steady-state oscillator excitation analysis by Breuhaus [28] and Milliken [29, 30] and also the pulse input method utilizing Fourier analysis [31] are examples of the frequency response method, which increased in popularity for aircraft analysis during the 1940s and 1950s. These methods produced the frequency response of the vehicle, but not the stability and control derivatives of the differential equations. Greenberg [32] and Shinbrot [33] attempted to extract those parameters by defining the values of the aircraft parameters that resulted in the best fit of the frequency response. Weighted least-square [33] and linear least-squares [34] techniques were also applied to flight data in the 1960s. But these techniques give poor results in the presence of measurement noise and yield biased estimates. Also, they are time consuming and singularities are a serious problem with them. The response curve-fitting technique [35] was formulated in 1951, which is equivalent to the output error technique. But due to the lack of efficient and faster computational means it did not work at that time.

In the 1950s and 1960s, time-vector methods [36-40] were commonly applied graphical procedures to determine aircraft parameters from flight data. However, those

methods give an incomplete set of parameters and only the responses of fairly simple motion can be analyzed. In the early 1960s, before the invention of digital computers, analog matching techniques [40, 41] which are time consuming and somewhat tedious, were applied to flight data. Resulting estimates differed depending on the skill and knowledge of the person. Discussion of these past techniques concluded that a more complete method of identification was needed, which can be faster and gives better results.

Two separate articles [42, 43] on output error methods for obtaining aerodynamic coefficients were published in the 1968. Taylor, Lawrence and Iliff [42] discussed the maximum-likelihood estimator for obtaining a complete set of aerodynamic parameters from flight data. Larson and Fleck [43] described a quasi-linearization method for parameter identification of an aircraft. This research had produced an excellent model which sufficiently described the resulting motion of the aircraft; which is the reason for the success of these two methods. Due to these two studies on aircraft identification using nonlinear minimization techniques, the interest in analysis of flight data was increased. After only a year in the 1969, Taylor and Iliff [44] modified these two techniques to include prior information. Minimization of this modified cost function does not result in a maximum-likelihood estimator because it was based on the joint probability distribution rather than the conditional probability [45]. Some excellent and very successful computer algorithms on system identification have been published

[46-50]. The maximum likelihood estimator method was found very useful for flight dynamic response [47-55].

Mehra [51] applied the Kalman filter to estimate aircraft aerodynamic parameters, which produced poor results, because the state estimation and parameter estimation were both biased. Hence, they did not converge to good results. Taylor, Powell and Mehra [56] obtained better results after addition of the derivative of the state. In the Netherlands, two successful applications of the Kalman filter, providing the state estimation and aircraft parameters identification were obtained [57, 58].

2. **Non-Deterministic Analysis:** There are two types of techniques applied for parameter estimation with measurement and state noise: the Kalman filter technique [51, 56-62] and maximum-likelihood estimator technique [52, 53, 63-65]. In the case of non-deterministic analysis, the maximum likelihood estimator technique is normally known as the filter error method. It was after 1965 that Astrom [59] and Kashyap [60] described general applications of the extended Kalman filter. During 1970, for the discrete-time system Taylor, Powell and Mehra [56] applied the extended Kalman filter to simulated aircraft data with a state noise input. Chen and Eulrich [61] experimented with an application to that of Taylor, Powell and Mehra in 1971, but it produced inconclusive results, as the state noise input was small, and also due to nonlinearity of the system. Yazawa [62] produced very good results, when he applied a simplified extended Kalman filter.

Iliff [65] applied the maximum-likelihood technique to output data of an aircraft flying in atmospheric turbulence. The results were similar for the same aircraft flying in smooth air, which is without state noise.

1.3.4 Latest Techniques of System Identification

The maximum likelihood estimator technique is used in most of the latest techniques of system identification. One of these methods, the filter error technique is completely detailed in Chapter 3. The digital computers of the modern era have the speed to implement self-regulating and self-governing data processing capability, which has changed the concentration of flight test data analysis utilizing methods based on frequency domain to methods based on time domain. Using modern computers, relatively larger numbers of aircraft stability and control derivatives can be estimated from only a single aircraft test. A coordinated approach based on flight test instrumentation, flight test techniques, and methods of data analysis gradually evolved for system identification as applied to aircraft [19, 46]:

1. **Instrumentation and filters**, which cover the entire flight data acquisition process including adequate instrumentation and airborne or ground-based digital recording equipment. Effects of all kinds of data quality should be accounted.
2. **Flight test techniques**, which are related to the selected flight vehicle maneuvering procedures. The input signals should be optimized in their spectral composition to excite all response modes from which parameters are to be estimated.

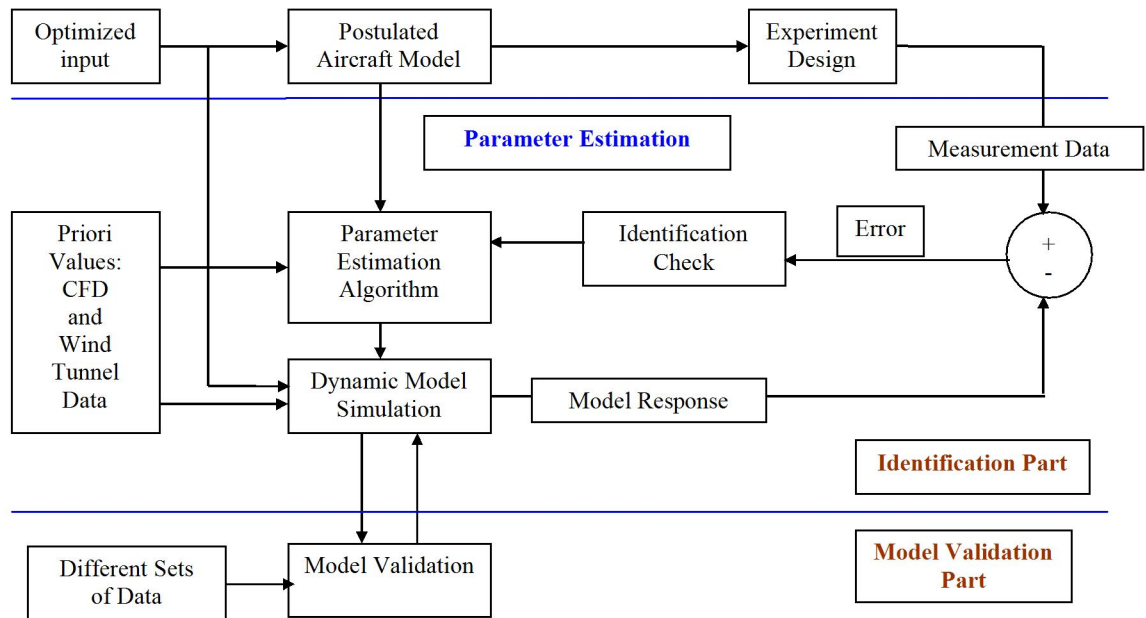


Figure 1.1: Block Diagram for System Identification to aircraft [1]

3. **Analysis of flight data**, which includes the mathematical model of the flight vehicle and an estimation criterion that devises a suitable computational algorithm to adjust starting values or *a priori* estimates of the unknown parameters until a set of best parameter estimates is obtained that minimizes the response error.

Synchronizing these interdependent subjects, four important aspects (Fig. 1.1) of the art and science of system identification have to be carefully treated:

1. design of the control input shape to excite all modes of the vehicle dynamic motion
2. selection of instrumentation and filters for high accuracy measurements
3. type of flight vehicle under investigation to define the structure of a possible mathematical model

4. the quality of data analysis by selecting the most suitable time or frequency domain identification method

The above four points must be followed carefully while investigating each aircraft. If they are followed, modern system identification methods for aircraft can generally be expected to provide good results. The modern techniques of data analysis for parameter estimation are classified as: 1) Equation error technique, 2) Output error technique, 3) Filter error technique. The last technique has been chosen for this study and is discussed in Chapter 3.

System identification is a multidisciplinary technique, which covers the fields of control theory, numerical techniques, theories of statistics, sensors and instrumentation, flight test techniques, signal processing, and flight dynamics. Basic knowledge of each of these fields enables the user to generate efficient results.

CHAPTER 2

BACKGROUND AND THEORETICAL DEVELOPMENT

Dynamical systems can generally be characterized by differential equations, whose order is dependent on the complexity of the whole process. The system identification process starts with postulating a model, so that it becomes possible to estimate the parameters of state through simulation. Usually this is done by solving an initial value problem utilizing numerical integration techniques. For system identification of aircraft, state space dynamical models characterizing the aircraft motion are usually used. These models are derived from Newtonian mechanics; which gives well formulated kinematic equations of aircraft motion with translational and rotational degrees of freedom [66].

2.1 Dynamical Model Description

As stated earlier, the system identification process for aircraft starts with postulating a dynamical model and governing equations of aircraft motion. The equations of motion also include the output and measurement equations. The complete set of equations is then [66]:

$$\begin{aligned}\dot{x} &= f[x(t), u(t), \zeta] + F(\vartheta)w(t), & x(t_0) &= x_0 \\ y &= g[x(t), u(t), \zeta] \\ z(t_k) &= y(t_k) + Gv(t_k)\end{aligned}\tag{2.1}$$

where x is the $(n \times 1)$ state vector, u is the $(s \times 1)$ input vector, y is the $(m \times 1)$ observation vector and z is the $(m \times 1)$ measurement vector. The unknown parameter vector Φ is given as:

$$\Phi = [\zeta^T \quad \vartheta^T \quad x_0^T]^T \quad (2.2)$$

In this specific case of system identification to aircraft, the system parameter vector ζ is made up of aircraft stability and control derivatives. The above nonlinear dynamical model can be linearized if required, using numerical approximation.

2.2 Cost Function (Performance Index) J

Using the measurement vector $z(t)$, observation vector $y(t)$, measurement noise covariance matrix R ($m \times m$), for n_y observation variables and N data points, a cost function, or performance index, J can be defined as follows [67].

$$J(\Phi, R) = \frac{1}{2} \int_1^N [z(t) - y(t)]^T R^{-1} [z(t) - y(t)] dt + \frac{N}{2} \ln [\det(R)] + \frac{N n_y}{2} \ln \det(2\pi) \quad (2.3)$$

where Φ is a column vector of parameters, which are to be estimated.

2.3 Essentials of Cost Function Minimization

For any experiment, the number of observations n_y and number of data points N shall be fixed. So, the last term in the above equation is a constant and hence can be neglected

without affecting the results [1]. Now for the measurement noise covariance matrix R , there are only two possibilities.

1. Known Measurement Noise Covariance Matrix R : Based on previous flight tests or using wind tunnel data, the measurement noise covariance matrix R can be assumed for this experiment. In this case, the second term in the above equation is constant. Then the cost function is simplified as [68].

$$J(\Phi) = \frac{1}{2} \int_1^N [z(t) - y(t)]^T R^{-1} [z(t) - y(t)] dt \quad (2.4)$$

Therefore, the cost function is easy to calculate and also quadratic in nature. It can be reduced using modern optimization methods given in the next section.

2. Unknown Measurement Noise Covariance Matrix R : Jategaonkar [1] used a relaxation strategy in which optimization of the likelihood function, Eq. 2.3 was carried out in two steps. In the first step, differentiate Eq. 2.3 partially with respect to R , set it equal to zero and derive

$$R = \frac{1}{N} \int_1^N [z(t) - y(t)] [z(t) - y(t)]^T dt \quad (2.5)$$

Substituting the value of R , obtained in Eq. 2.5 in Eq. 2.3 will give the result:

$$J(\Phi) = \frac{1}{2} n_y N + \frac{N}{2} \ln [\det(R)] + \frac{N n_y}{2} \ln \det(2\pi) \quad (2.6)$$

The first term and the last term on the right side of the above equation are constant because N and n_y are fixed for any model. Therefore, without affecting the minimization results the cost function reduces to [1]:

$$J(\Phi) = \det(R) \tag{2.7}$$

Now, the value of parameter vector Φ is to be determined, which should minimize $\det(R)$, that is the cost function. The elements of Φ may be determined as per the requirement by a variety of optimization techniques. A relaxation strategy will be followed in this thesis, as outlined below.

1. Assume parameter vector Φ with suitable initial values.
2. Determine system observation (or output) matrix Y . Compute the innovation vector $(Z - Y)$. Determine measurement noise covariance matrix R .
3. Calculate cost function J .
4. Apply any of the optimization techniques to reduce Cost function J .
5. Repeat the algorithm from step 2 to step 4 until the cost function reduces satisfactorily and also, the estimates converge to a specific and constant values.

Numerous optimization techniques have been developed for linear and nonlinear optimization. Direct search techniques, accelerated gradient based techniques and modified Newton-Raphson techniques [69] are few of them. In this thesis the modified Newton-Raphson technique is utilized.

2.4 Modified Newton-Raphson Algorithm

The Newton-Raphson technique is an iterative method, which finds a zero of the gradient of a cost function, that is

$$\frac{\partial J(\Phi)}{\partial \Phi} = 0 \quad (2.8)$$

$\frac{\partial J}{\partial \Phi}$ is expanded using two-term Taylor's series about the i^{th} value of the parameter vector Φ :

$$\left(\frac{\partial J(\Phi)}{\partial \Phi}\right)_{i+1} \approx \left(\frac{\partial J(\Phi)}{\partial \Phi}\right)_i + \left(\frac{\partial^2 J(\Phi)}{\partial \Phi^2}\right)_i \Delta \Phi \quad (2.9)$$

where $\Delta \Phi = \Phi_{i+1} - \Phi_i$ is the parameter change and $\left(\frac{\partial^2 J(\Phi)}{\partial \Phi^2}\right)_i$ is the second derivative of the cost function with respect to Φ at the i^{th} iteration [68]. The change in Φ can be written

$$\Delta \Phi = - \left[\left(\frac{\partial^2 J}{\partial \Phi^2}\right)_i \right]^{-1} \left(\frac{\partial J}{\partial \Phi}\right)_i \quad (2.10)$$

The Newton-Raphson algorithm described above, is more efficient than the gradient method because it attempts to predict where the local minimum point is quadratically convergent [69, 70]. To compute the first gradient of the cost function, Eq. 2.3 can be partially

differentiated with respect to Φ and the result is:

$$\frac{\partial J}{\partial \Phi} = - \int_1^N \left[\frac{\partial y(t)}{\partial \Phi} \right]^T R^{-1} [z(t) - y(t)] dt \quad (2.11)$$

Differentiating the above equation with respect to Φ , the second gradient matrix can be formed as [68]:

$$\frac{\partial^2 J}{\partial \Phi^2} = \int_1^N \left[\frac{\partial y(t)}{\partial \Phi} \right]^T R^{-1} \left[\frac{\partial y(t)}{\partial \Phi} dt \right] + \int_1^N \left[\frac{\partial^2 y(t)}{\partial \Phi^2} \right]^T R^{-1} [z(t) - y(t)] dt \quad (2.12)$$

The first gradient of the cost function can be calculated easily but computation of the second gradient is complicated and time consuming. The prime reason for this complexity is the computation of the second gradient of the response $\frac{\partial^2 y}{\partial \Phi^2}$, which is found in the second integral of Eq. 2.12. Balakrishnan [71] suggested a simplification as follows. The second term of Eq. 2.12 goes to zero as the process converges. Hence, it can be neglected and the second gradient can be approximated as:

$$\frac{\partial^2 J}{\partial \Phi^2} = \int_1^N \left[\frac{\partial y(t)}{\partial \Phi} \right]^T R^{-1} \left[\frac{\partial y(t)}{\partial \Phi} dt \right] \quad (2.13)$$

This yields a more flexible technique called the modified Newton-Raphson method. This technique is also referred to as the Newton-Balakrishnan method or Gauss-Newton method.

This leads to a system of linear equations that can be summarized as follow [68]:

$$\text{Denote } P1 = - \left[\left(\frac{\partial^2 J}{\partial \Phi^2} \right)_i \right]^{-1} \quad \text{and} \quad P2 = \left(\frac{\partial J}{\partial \Phi} \right)_i \quad (2.14)$$

From Eq. 2.11 and Eq. 2.13:

$$P1 = \int_1^N \left[\frac{\partial y(t)}{\partial \Phi} \right]^T R^{-1} \left[\frac{\partial y(t)}{\partial \Phi} dt \right] \quad (2.15)$$

$$P2 = - \int_1^N \left[\frac{\partial y(t)}{\partial \Phi} \right]^T R^{-1} [z(t) - y(t)] dt \quad (2.16)$$

Then,

$$\Phi_{i+1} = \Phi_i + \Delta \Phi, \quad \text{where} \quad \Delta \Phi = -P1^{-1}P2 \quad (2.17)$$

CHAPTER 3

SYSTEM IDENTIFICATION OF GENERAL AVIATION AIRCRAFT

The various aircraft parameter estimation techniques are:

1. The equation error technique
2. The output error technique
3. The filter error techniques
4. The frequency domain techniques
5. The recursive parameter estimation technique
6. The artificial neural network based techniques

A filter error technique is used in this thesis. The filter error techniques represent the general stochastic approach to aircraft system identification introduced by Balakrishnan [63]. Iliff [65] and Mehra [51, 56, 72] utilized these techniques in the 1970s. These techniques are highly efficient while working with measurement and process noise.

3.1 Filter Error Technique for Linear Systems

A block diagram of the filter error technique is shown in Fig. 3.1. In this section, the filter error technique for linear systems will be discussed with theoretical advancements and computational aspects.

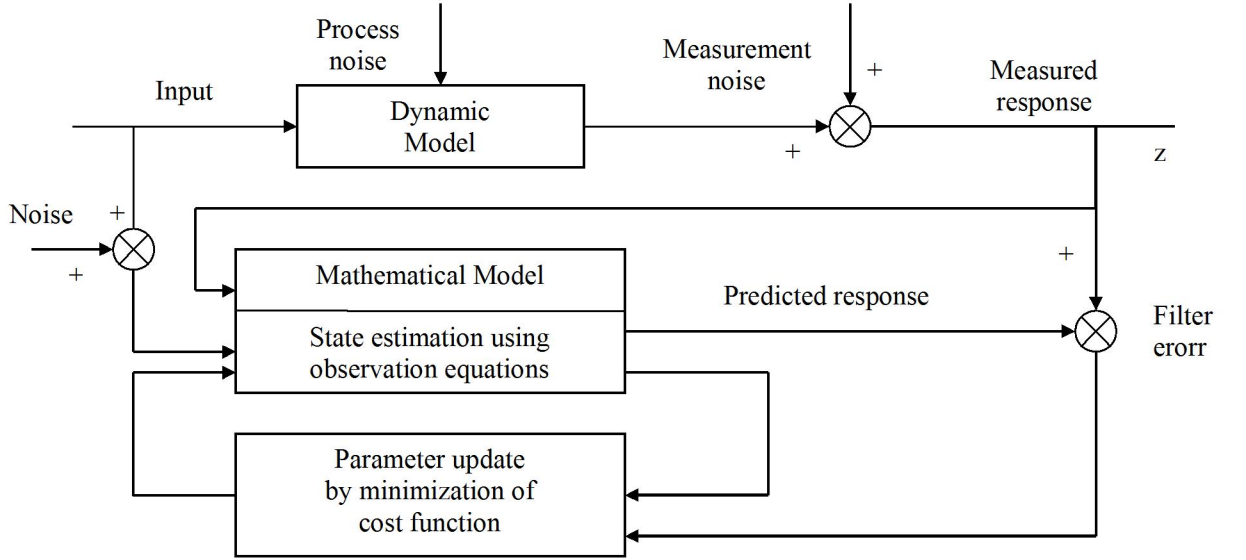


Figure 3.1: Block Diagram for Filter Error Technique [68]

A dynamic system can be described by the following stochastic linear mathematical model [1].

$$\dot{x}(t) = Ax(t) + Bu(t) + Fw(t) + b_x, \quad x(t_0) = 0 \quad (3.1)$$

$$y(t) = Cx(t) + Du(t) + b_y \quad (3.2)$$

$$z(t_k) = y(t_k) + Gv_k, \quad k = 1, 2, \dots, N \quad (3.3)$$

where x is a state vector ($n \times 1$), u is a control input vector ($s \times 1$), y is an output vector ($m \times 1$), and z is a measurement vector ($m \times 1$) sampled at N discrete time points. Matrices A ($n \times n$), and C ($m \times n$), contain unknown stability derivatives and matrices B ($n \times s$), and D ($m \times s$), contain unknown control derivatives. Matrices F ($n \times n$), and G ($m \times m$), represent

the process and measurement noise distribution matrices, respectively. In the state and observation equations, b_x and b_y are bias terms. In the most general case all of the elements of the matrices A , B , C , D and bias terms, b_x and b_y form the parameter vector Φ , which is to be estimated.

From the Eqs. 2.3-2.4, output vector, y , is required now, to calculate the cost function J and the measurement noise covariance matrix, R . A Kalman filter is used to estimate the output vector given the observed data, Z_{t_k} . Parameter estimates for Φ and R are obtained by minimizing the cost function.

Though it can be assumed that the process and measurement noises are additive, the estimation process is still complicated because the nature of the system is non-deterministic [67]. Because of the process and measurement noise, it is not possible to integrate the state equations. Instead, a standard Kalman filter is utilized as an optimal state estimator for the linear system [73, 74].

3.1.1 Kalman Filter

The Kalman filter consists of two steps, a prediction and a correction step.

1. **Prediction step:** For the linear model postulated in Eqs. 3.1-3.2, the prediction step is given by [1]:

$$\tilde{x}(t_{k+1}) = \Theta \hat{x}(t_k) + \Lambda B \bar{u}(t_k) + \Lambda b_x \quad (3.4)$$

$$y(t_k) = C \tilde{x}(t_k) + D u(t_k) + b_x \quad (3.5)$$

2. Correction step

$$\hat{x}(t_k) = \tilde{x}(t_k) + K[z(t_k) - y(t_k)] \quad (3.6)$$

Here, \tilde{x} is a predicted state vector, \hat{x} is a corrected state vector, \bar{u} is an average of the control input at two successive discrete time steps, \tilde{y} is a predicted observation vector and $[z(t_k) - \tilde{y}(t_k)]$ is the residual (or innovation). Θ and Λ are the state transition matrix and integral of state transition matrix (derived in appendix A). K is the Kalman gain ($n \times m$) and is dependent on the observation matrix C , state prediction error covariance matrix P ($n \times n$), and measurement error covariance matrix R ($m \times m$), and given as [67]:

$$K = PC^T R^{-1} \quad (3.7)$$

The measurement noise covariance matrix R can be found using Eq. 2.5 and the state prediction error covariance matrix P is calculated by solving the Riccati equation.

3.1.2 Solution of Riccati Equation

The Riccati equation is solved to compute the state prediction error covariance matrix, P . A steady-state form of the continuous-time Riccati equation is used here because it is easier than the discrete-time equation [1, 67, 75]. The first order projection of the Riccati equation is given below.

$$AP + PA^T - \frac{1}{\Delta t} PC^T R^{-1} CP + FF^T = 0 \quad (3.8)$$

Eq. 3.8 can be solved using Potter's method [1, 76] based on eigenvector decomposition. Only the necessary details are provided here. Solution of the Riccati equation follows three steps and is very straightforward.

1. Start with formulation of the Hamiltonian matrix, H , as [67]:

$$H = \left[\begin{array}{c|c} A & -FF^T \\ \hline -\frac{1}{\Delta t}C^TR^{-1}C & -A^T \end{array} \right] \quad (3.9)$$

2. Compute the eigenvalues and eigenvector of the Hamiltonian matrix, H . Divide the eigenvector matrix into four equal size matrices such that the eigenvectors related to eigenvalues with positive real parts remain on the left side. Controllability due to process noise and observability ensure that exactly one half of the eigenvectors will have positive real parts (i.e., unstable eigenvalues). Suppose M is the eigenvector matrix of H , then it can be divided and arranged as [67]:

$$M = \left[\begin{array}{c|c} M_{11} & M_{12} \\ \hline M_{21} & M_{22} \end{array} \right] \quad (3.10)$$

3. The solution of the steady-state, continuous-time Riccati equation is as follows [67]:

$$P = -M_{11}M_{21}^{-1} \quad (3.11)$$

The state prediction error covariance matrix, P , is a steady-state matrix and is not dependent on time [1].

3.1.3 Formulations for Process Noise

Three principle formulations have been used to account for both the process and measurement noises based on the way the measurement noise covariance matrix, R ; Kalman gain matrix, K ; and the noise distribution matrices, F and G , are estimated [54, 67, 68].

1. Natural Formulation

The natural formulation [67, 68] utilizes the unknown parameter vector Φ in the best possible optimization method and minimizes the cost function. The elements of parameter vector Φ are all or some elements of matrices the A , B , C , D , F , G . This formulation is very easy to define and theoretically a possible and perfect technique. But, if the problem considered has process and measurement noises, this formulation is not a practical one. Mainly because this formulation does not have an explicit solution to estimate the noises. There are three primary disadvantages of this formulation, primarily due to the complications in the estimation of F and G matrices. The drawbacks are convergence, singularity and computational burden. Therefore, this technique is not used extensively these days.

2. Innovation Formulation

The innovation formulation was suggested to overcome the difficulties of the natural formulation. It is very similar to the formulation which was followed in the output error method [51, 62, 67]. As it was mentioned in the previous section, the prime difficulty of the natural formulation is estimation of the F and G matrices. From the definitions of the cost function, J , in Eq. 2.3 and measurement noise covariance matrix, R , in Eq. 2.5, it is clear that they are dependent on the F and G matrices indirectly through the

Kalman gain. Therefore, if the Kalman gain is directly estimated, then the complications due to the natural formulation would be solved. In this case, the elements of the parameter vector Φ are all or some elements of the matrices A , B , C , D , K . This formulation works well with process and measurement noises and also for linear and nonlinear systems. The straightforward solution of the cost function, J , from Eq. 2.6 and measurement noise covariance matrix, R , in Eq. 2.5 solves the convergence problems.

Because the innovation formulation estimates the Kalman gain K directly (in place of deriving the same from Eq. 3.7, it solves the remaining parameter estimation problem utilizing only three equations (3.4-3.6). The best part of this formulation is it excludes the need to compute the most complex part of the algorithm, that is the solution of the Riccati equation. Thus, this technique looks more appealing computationally, however, it has a few disadvantages [67]. The size of matrix K is larger than that of matrix F . The parameter vector Φ is larger here, which takes more computational time. The elements of K do not have direct physical meaning [68]. Moreover, the Kalman gain, K as well as system parameters and measurement noise covariance matrix, R , are computed separately, which may give unsuitable estimates for R and K .

3. Combined Formulation

Maine and Iliff [55, 67] proposed a Combined Formulation in 1981, which takes the best features from both of the previous formulations. The combined formulation estimates the process noise matrix, F , and it calculates the measurement noise covariance matrix, R , from Eq. 2.5. Hence, the parameter vector, Φ , consists of all or some elements of the matrices A ,

B , C , D , F , and a two-step relaxation strategy is applied. Here the first step is to estimate the measurement noise covariance matrix, R , which is relatively simpler. The Parameter vector, Φ , is estimated in the second step utilizing the modified Newton-Raphson technique. The primary advantage of this method is that the process noise matrix, F , has a physical meaning. To estimate the state prediction error covariance matrix, P , the solution of the Riccati equation is necessary. Although this solution is tedious, it is worthwhile because the results of this formulation are more practical with respect to convergence, singularities, parameter estimates and computation burden [1].

3.1.4 The Filter Error Algorithm for Linear Systems

After comparing the three formulations, only the combined formulation is followed in this thesis due to its inherent efficiency. The filter error algorithm for linear systems is outlined in Fig. 3.2. In this technique the following tasks are important.

1. Select suitable initial values for the unknown parameter vector, Φ , the Kalman gain, K , the state prediction error covariance matrix, P , and states x . Load the available flight data (from real time flight or from a simulator).
2. Apply the Kalman filter and calculate the observation vector, Y ; innovation matrix, initial measurement noise covariance matrix, R ; and based on that the initial cost function, J .
3. Solve the Riccati equation and find the new Kalman gain. Calculate the new measurement noise covariance matrix, R , and based on that the new cost function, J .

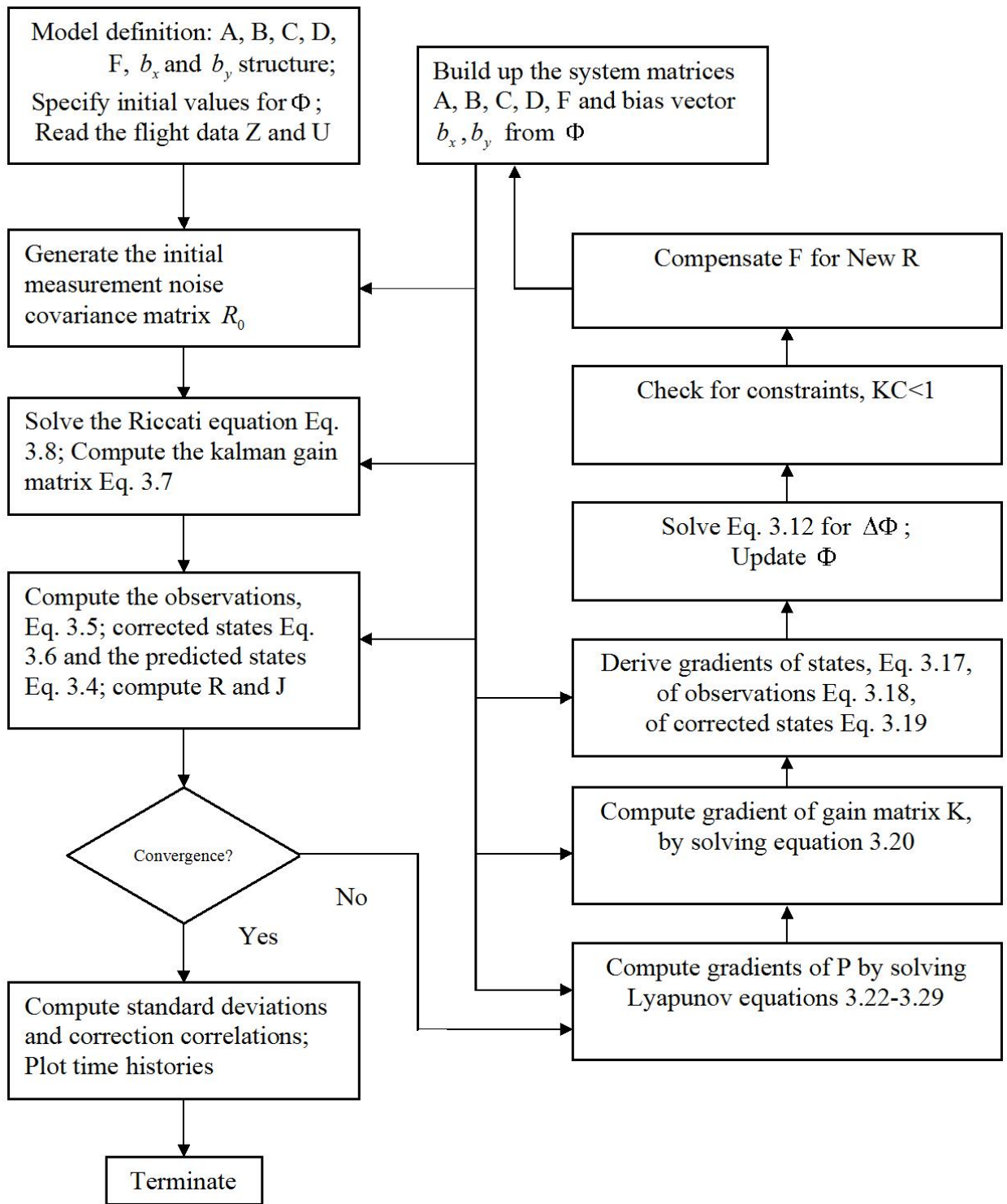


Figure 3.2: Algorithm of Filter Error Technique for Linear Systems [1]

4. Apply the modified Newton-Raphson technique to minimize the cost function.
5. Update the parameter vector Φ .
6. Repeat the steps 3-5 until all parameters converge to specific and constant values.

3.1.5 Parameter Update

The modified Newton-Raphson method is applied in this section to update the parameter vector, Φ , such that it minimizes the cost function after each iteration. The following equations were derived in section 2.4 [1].

$$\Phi_{i+1} = \Phi_i + \Delta\Phi, \quad \text{where} \quad \Delta\Phi = -P1^{-1}P2 \quad (3.12)$$

$$P1 = \int_1^N \left[\frac{\partial y(t_k)}{\partial \Phi} \right]^T R^{-1} \left[\frac{\partial y(t_k)}{\partial \Phi} dt \right] \quad (3.13)$$

$$P2 = -\int_1^N \left[\frac{\partial y(t_k)}{\partial \Phi} \right]^T R^{-1} [z(t_k) - y(t_k)] dt \quad (3.14)$$

In the above equations, everything is readily available to use, except the sensitivity matrix or the gradient matrix of response, given below [1]:

$$\left(\frac{\partial y}{\partial \Phi} \right)_{ij} = \frac{\partial y_i}{\partial \Phi_j} \quad (3.15)$$

The sensitivity matrix $\left(\frac{\partial y}{\partial \Phi} \right)$ can be solved using several ways. However, the classical method is used in this thesis by solving the sensitivity equations [69]. The finite difference method is also an excellent method, which is usually applied for nonlinear system. The required

sensitivity equations are obtained by differentiating the system equations with respect to elements of the parameter matrix, Φ . Partial differentiation of Eq. 3.4 results in the following equation [1].

$$\frac{\partial \tilde{x}(t_{k+1})}{\partial \Phi} = \Theta \frac{\partial \hat{x}(t_k)}{\partial \Phi} + \frac{\partial \Theta}{\partial \Phi} \hat{x}(t_k) + \Lambda \frac{\partial B}{\partial \Phi} \bar{u}(t_k) + \frac{\partial \Lambda}{\partial \Phi} B \bar{u}(t_k) + \Lambda \frac{\partial b_x}{\partial \Phi} + \frac{\partial \Lambda}{\partial \Phi} b_x \quad (3.16)$$

The above equation is the exact gradient of Eq. 3.4 and is necessary to compute $\frac{\partial \Theta}{\partial \Phi}$ and $\frac{\partial \Lambda}{\partial \Phi}$. Maine and Iliff [67] eliminated this computation burden by approximating the gradient computation significantly, explained below:

$$\frac{\partial \tilde{x}(t_{k+1})}{\partial \Phi} \approx \Theta \frac{\partial \hat{x}(t_k)}{\partial \Phi} + \Lambda \frac{\partial A}{\partial \Phi} \bar{x}(t_k) + \Lambda \frac{\partial B}{\partial \Phi} \bar{u}(t_k) + \Lambda \frac{\partial b_x}{\partial \Phi}, \quad \frac{\partial \tilde{x}(1)}{\partial \Phi} = 0 \quad (3.17)$$

Two new terms are introduced in the above equations. An average of two consecutive inputs is shown as \bar{u} and \bar{x} is an average of states at two successive time steps. Partial differentiation of Eq. 3.5 and Eq. 3.6 result in the following equation [67].

$$\frac{\partial y(t_k)}{\partial \Phi} = C \frac{\partial \tilde{x}(t_k)}{\partial \Phi} + \frac{\partial C}{\partial \Phi} \tilde{x}(t_k) + \frac{\partial D}{\partial \Phi} u(t) + \frac{\partial b_y}{\partial \Phi} \quad (3.18)$$

$$\frac{\partial \hat{x}(t_k)}{\partial \Phi} = \frac{\partial \tilde{x}(t_k)}{\partial \Phi} - K \frac{\partial y(t_k)}{\partial \Phi} + \frac{\partial K}{\partial \Phi} [z(t_k) - y(t_k)] \quad (3.19)$$

Eqs. 3.17-3.19 represent a set of sensitivity equations. Except for the $\frac{\partial K}{\partial \Phi}$ all terms are available at this point. Therefore, the gradient of the Kalman gain matrix is computed to complete this optimization problem. Differentiate Eq. 3.7 to derive the following result

[67].

$$\frac{\partial K}{\partial \Phi} = \frac{\partial P}{\partial \Phi} C^T R^{-1} + P \frac{\partial C^T}{\partial \Phi} R^{-1} \quad (3.20)$$

For each specific time step and at this stage in the algorithm measurement noise covariance matrix R , system matrix C and state prediction error covariance matrix P are fixed and constant. Partial differentiation of each element matrix C with respect to related parameters is one and elsewhere it is zero. Thus, only $\frac{\partial P}{\partial \Phi}$ needs to be calculated to compute the gradient of K . Note that $\frac{\partial P}{\partial \Phi}$ is a three dimensional matrix and hence $\frac{\partial K}{\partial \Phi}$ is also a three dimensional matrix. $\frac{\partial P}{\partial \Phi}$ is derived by differentiating the steady-state Riccati equation 3.8 [67].

$$\begin{aligned} A \frac{\partial P}{\partial \Phi} + \frac{\partial A}{\partial \Phi} P + P \frac{\partial A^T}{\partial \Phi} + \frac{\partial P}{\partial \Phi} A^T - \frac{1}{\Delta t} \frac{\partial P}{\partial \Phi} C^T R^{-1} C P - \frac{1}{\Delta t} P \frac{\partial C^T}{\partial \Phi} R^{-1} C P \\ - \frac{1}{\Delta t} P C^T R^{-1} \frac{\partial C}{\partial \Phi} - \frac{1}{\Delta t} P C^T R^{-1} C \frac{\partial P}{\partial \Phi} + F \frac{\partial F^T}{\partial \Phi} + \frac{\partial F}{\partial \Phi} F^T = 0 \end{aligned} \quad (3.21)$$

Arrange the left-hand side terms and simplify mathematically using matrix properties like $(A + B)^T = A^T + B^T$ and $(AB)^T = B^T A^T$. The result is shown here [67].

$$\bar{A} \frac{\partial P}{\partial \Phi} + \frac{\partial P}{\partial \Phi} \bar{A}^T = \bar{C} + \bar{C}^T \quad (3.22)$$

where

$$\bar{A} = A - \frac{1}{\Delta t} P C^T R^{-1} C = A - \frac{1}{\Delta t} K C \quad (3.23)$$

and

$$\bar{C} = -\frac{\partial A}{\partial \Phi} P + \frac{1}{\Delta t} P C^T R^{-1} \frac{\partial C}{\partial \Phi} P - \frac{\partial F}{\partial \Phi} F^T \quad (3.24)$$

There is one equation like Eq. 3.22 for each element of the system parameter vector Φ . This leads to a set of Lyapunov equations of the form $AX + XA^T = B$ [1, 67]. Since the \bar{A} matrix remains similar for the entire set, the Lyapunov equations are solved efficiently utilizing the following transformation [67].

$$\bar{A}' = T^{-1}\bar{A}T \quad (3.25)$$

and

$$(\bar{C} + \bar{C}^T)' = T^{-1}(\bar{C} + \bar{C}^T)T^{*-1} \quad (3.26)$$

Here, T is the matrix of the eigenvectors of \bar{A} . Due to this alteration \bar{A}' is now diagonal and thus Eq. 3.22 is left as [67]:

$$\bar{A}' \left(\frac{\partial P}{\partial \Phi} \right)' + \left(\frac{\partial P}{\partial \Phi} \right)' \bar{A}'^* = (\bar{C} + \bar{C}^T)' \quad (3.27)$$

As the \bar{A}' is diagonal, the above equation can be solved for $\left(\frac{\partial P}{\partial \Phi} \right)'$ easily. Generally for a diagonal matrix A , $AX + XA^T = B$ can be solved by [67]

$$X_{ij} = \frac{B_{ij}}{(A_{ii} + A_{jj})} \quad (3.28)$$

The gradient of the state prediction error covariance matrix P is calculated using back transformation [67].

$$\frac{\partial P}{\partial \Phi} = T \left(\frac{\partial P}{\partial \Phi} \right)' T^* \quad (3.29)$$

Now, Eqs. 3.12-3.14 can be solved easily. As stated earlier, this technique leads to an unconditional minimum of the cost function. All system parameters are treated separately. The results obtained using this technique will be provided and discussed in the next chapter.

3.2 Filter Error Technique for Non-linear Systems

The general mathematical model of a non-linear system is given below:

$$\dot{x}(t) = f[x(t), u(t), \beta] + Fw(t), \quad x(t_0) = x_0 \quad (3.30)$$

$$y(t) = g[x(t), u(t), \beta] \quad (3.31)$$

$$z(t_k) = y(t) + Gv(t_k) \quad (3.32)$$

Here f and g are nonlinear functions, $x(t)$ is a state vector and $u(t)$ is an input vector. F and G are time-invariant noise distribution matrices.

The filter error technique for nonlinear systems is illustrated in Fig. 3.3. For non-linear systems, response gradients are calculated based on finite difference approximations. An extended Kalman filter [77, 78] dependent on the first-order approximation of the dynamical equations is used for non-linear filtering.

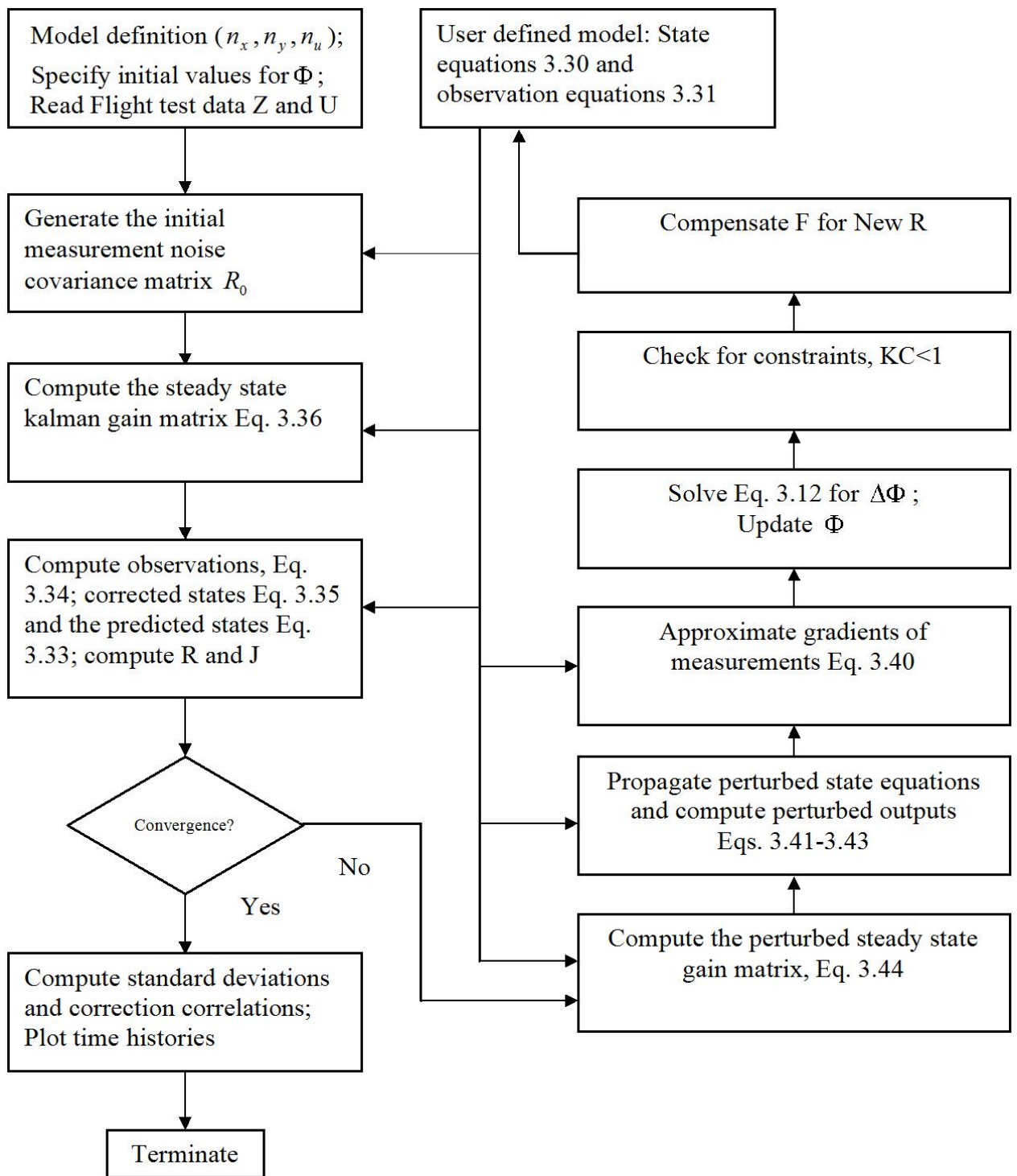


Figure 3.3: Algorithm of Filter Error Technique for Nonlinear Systems [1]

3.2.1 Steady State Filter

The combined formulation is followed, for the nonlinear case just as was done for the linear case. The two-step relation strategy, discussed in section 2.4 is applied to estimate R . While doing this, the following tasks are important.

1. Select some suitable initial values for the unknown parameter vector Φ . Load the available flight data (from real time flight or from simulator).
2. Apply the extended Kalman filter and calculate the observation vector, Y ; innovation matrix; initial measurement noise covariance matrix, R ; and the initial cost function, J . Numerically integrate the state equations. For numerical integration, a fourth order Runge-Kutta method was used. A description of this method is given in appendix B.
3. Solve the Riccati equation and find the new Kalman gain. Calculate a new measurement noise covariance matrix, R , and new cost function, J .
4. Apply the modified Newton-Raphson technique to minimize the cost function.
5. Update the parameter vector, Φ .
6. Repeat steps 3-5 until all parameters converge to constant values.

The optimal filters are practically impossible for non-linear systems. Hence, an extended Kalman filter is used here. A two-step, non-linear, constant-gain filter is formulated as [1].

Prediction step

$$\tilde{x}(t_{k+1}) = \hat{x}(t_k) + \int_{t_k}^{t_{k+1}} f[x(t), \bar{u}(t), \beta] dt, \quad \hat{x}(t_0) = x_0 \quad (3.33)$$

$$y(t_k) = g[\tilde{x}(t), u(t), \beta] \quad (3.34)$$

Correction step

$$\hat{x}(t_k) = \tilde{x}(t_k) + K[z(t_k) - y(t_k)] \quad (3.35)$$

The Kalman gain K is dependent on the measurement noise covariance matrix, R , state prediction error covariance matrix, P ; and system matrix, C . It is expressed as [1]:

$$K = PC^T R^{-1} \quad (3.36)$$

where

$$C = \left[\frac{\partial g[x(t), u(t), \beta]}{\partial x} \right]_{t=t_0} \quad (3.37)$$

A steady-state, continuous-time, Riccati equation is solved here to calculate P . The linearized matrices A and C are used, and solved using a finite difference method which is explained below.

Finite Difference Technique:

If each of the state variables is perturbed by δx_j , the elements of the matrices A and C can be approximated using a central difference formula as [1]:

$$A_{ij} \approx \left(\frac{f_i[x + \delta x_j, u, \beta] - f_i[x - \delta x_j, u, \beta]}{2\delta x_j} \right)_{x=x_0} \quad (3.38)$$

$$C_{ij} \approx \left(\frac{g_i[x + \delta x_j, u, \beta] - g_i[x - \delta x_j, u, \beta]}{2\delta x_j} \right)_{x=x_0} \quad (3.39)$$

For the non-linear system, the response gradients are approximated using the finite difference approximation. For a small perturbation $\delta\Phi_j$ in each variable of the unknown parameter vector Φ , the perturbed response variable y_p for each of the unperturbed variable y_i is computed. The sensitivity response gradient is approximated as

$$\left[\frac{\partial y(t_k)}{\partial \Phi} \right] = \frac{y_p(t_k) - y_i(t_k)}{\delta\Phi} \quad (3.40)$$

For each element of the unknown parameter vector, Φ , the state and observation variables are calculated utilizing a two step non-linear steady-state filter as given below [1].

Prediction step

$$\tilde{x}_{p-j}(t_{k+1}) = \hat{x}_{p-j}(t_k) + \int_{t_k}^{t_{k+1}} f[x_{p-j}(t_{k+1}), \bar{u}(t_{k+1}), \beta + \delta\beta_j e^j] dt \quad (3.41)$$

$$y_{p-j}(t_k) = g[\tilde{x}_{p-j}(t_{k+1}), u(t_{k+1}), \beta + \delta\beta_j e^j] \quad (3.42)$$

Correction step

$$\hat{x}_{p-j}(t_k) = \tilde{x}_{p-j}(t_k) + K_{p-j}[z(t_k) - y_{p-j}(t_k)] \quad (3.43)$$

The predicted state variables \tilde{x} in Eq. 3.41 are computed by numerical integration. To compute Eq. 3.43 the perturbed Kalman gain matrix K_{p-j} needs to be calculated, which is given by [1]

$$K_{p-j} = P_{p-j}C_{p-j}^TR^{-1} \quad (3.44)$$

here, the perturbed system matrices A_{p-j} and C_{p-j} need to be calculated to use them to solve the Riccati equation, which are approximated using a central difference method.

3.2.2 Parameter Update

Referring to section 3.1.5 and Eqs. 3.13-3.14, all quantities can be derived for non-linear systems. The parameter vector Φ will be updated using Eq. 3.12. This technique also leads to an unconditional minimum of the cost function. The results obtained using this technique will be provided and discussed in the next chapter.

CHAPTER 4

PREDICTION OF AIRCRAFT STABILITY AND CONTROL DERIVATIVES

Techniques to calculate the stability and control derivatives analytically, are presented in this chapter. These derivatives are an important part of the experiment because they are required as an input to determine dynamic stability and control behavior [79]. These methods are referred from [79-83]. Only preliminary information is presented here. Details should be found from [79-83]. Stability and control derivatives given in Eqs. 5.1-5.5 are predicted using the following methods. Initial values derived using these methods were used in the experimental aircraft Trainer.

The important notes while using these methods are [79]:

1. The methods presented in this chapter apply only to rigid aircraft.
2. The methods presented in this chapter apply only to subsonic speed regimes.
3. All derivatives are in rad^{-1} .
4. All coefficients and derivatives are defined in the stability axes system.
5. The drag prediction methods apply only in the flight cases where the boundary layer is turbulent.
6. The drag prediction methods apply only to smooth surfaces.

4.1 Steady State Coefficients

The definitions of steady state coefficients C_D , C_L and C_{m_0} are given below. They were used to determine the lift, drag and pitching moment steady state coefficients [79].

C_L is the aircraft's steady-state lift coefficient, given as [79]:

$$C_L = W/(\bar{q}S) \quad (4.1)$$

C_D is the aircraft's steady-state drag coefficient. It is calculated using the following method. As shown in Fig. 4.1, it is related to a specific value of steady-state lift coefficient C_L . The steady-state aircraft drag coefficient is given as follows [79]:

$$C_D = C_{D_w} + C_{D_{fus}} \quad (4.2)$$

The wing drag coefficient is predicted from [79]:

$$\begin{aligned} C_{D_w} &= C_{D_{0w}} + C_{D_{Lw}} \\ \text{where } C_{D_{0w}} &= (R_{wf})(R_{LS})(R_{fw})\{1 + L'(t/c) + 100(t/c)^4\}(S_{wet}/S) \\ \text{and } C_{D_{Lw}} &= (C_{L_w})^2/\pi Ae + 2\pi C_{L_w}\eta_t v + 4\pi^2(\eta_t)^2 w \end{aligned} \quad (4.3)$$

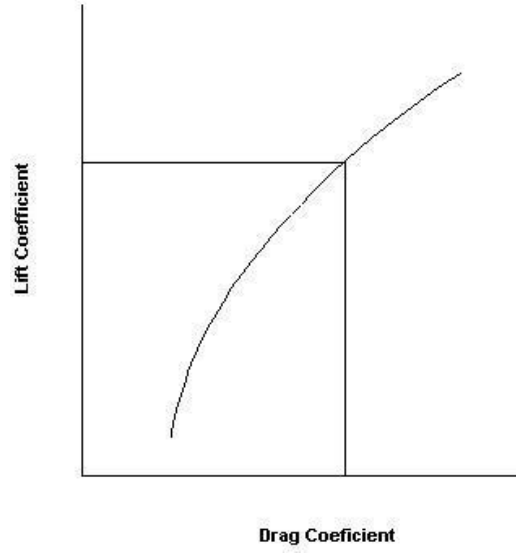


Figure 4.1: Determination of Drag Coefficient from a known Lift Coefficient

The fuselage drag coefficient is predicted from [79]:

$$C_{D_{fus}} = C_{D_{0_{fus}}} + C_{D_{L_{fus}}}$$

$$\text{where } C_{D_{0_{fus}}} = (R_{wf})(C_{f_{fus}})\{1 + 60(l_f/d_f)^3 + 0.0025(l_f/d_f)\}(S_{wet}/S) + C_{D_{b_{fus}}}$$

$$\text{and } C_{D_{L_{fus}}} = 2\alpha^2(S_b/S) + \eta c_{dc}\alpha^3(S_{pl,f_{fus}}/S) \quad (4.4)$$

C_{m_0} is the aircraft zero lift pitching moment coefficient and can be predicted using the following equation [79]:

$$C_{m_0} = C_{m_{0_{wf}}} + C_{m_{0_h}} \quad (4.5)$$

$C_{m_{0_{wf}}}$ is the zero lift pitching moment coefficient due to wing-fuselage combination. It is predicted from [79]:

$$C_{m_{0_{wf}}} = \{(C_{m_{0_w}}) + (C_{m_{0_f}})\} \{(C_{m_0})_M + (C_{m_0})_{M=0}\}$$

$$\text{where } C_{m_{0_w}} = \{(A \cos^2 \Lambda_{c/4}) / (A + 2 \cos \Lambda_{c/4})\} (c_{m_{0_r}} + c_{m_{0_t}}) / 2$$

$$+ (\Delta C_{m_0} / \epsilon_t) \epsilon_t$$

$$\text{and } C_{m_{0_f}} = \{(k_2 - k_1) / 36.5 S \bar{c}\} \left[\sum \{(w_{f_i}^2) (i_w + \alpha_{0_{L_w}} + i_{cl_f}) \Delta x_i \} \right] \quad (4.6)$$

$C_{m_{0_h}}$ is the zero lift pitching moment coefficient because of the horizontal tail. It is predicted from [79]:

$$C_{m_{0_h}} = -(\bar{x}_{ac_h} - \bar{x}_{ref}) C_{L_{0_h}} \quad (4.7)$$

4.2 Stability Derivatives

The techniques for calculating the following stability derivatives are addressed in this section:

1. Aircraft speed derivatives.
2. Angle of attack derivatives.
3. Angle of sideslip derivatives.
4. Roll rate derivatives.

5. Pitch rate derivatives.

6. Yaw rate derivatives.

As it was stated before, only preliminary equations are addressed here. Complete analysis can be found in [79-83].

4.2.1 Aircraft Speed Derivatives

The aerodynamic speed derivative C_{L_V} , lift with respect to aircraft speed is determined using the following equation [79].

$$C_{L_V} = \{M^2(\cos\Lambda_{c/4})^2 C_L\} / \{1 - M^2(\cos\Lambda_{c/4})^2\} \quad (4.8)$$

The aerodynamic speed derivative C_{D_V} , drag with respect to aircraft speed is determined using the following equation [79].

$$C_{D_V} = M(\partial C_D / \partial M) \quad (4.9)$$

The aerodynamic speed derivative C_{m_V} , pitching moment with respect to aircraft speed is determined using the following equation [79].

$$C_{m_V} = -C_L(\partial \bar{X}_{ac_A} / \partial M) \quad (4.10)$$

4.2.2 Angle of Attack Derivatives

The derivative of the aerodynamic lift with respect to aircraft angle of attack (also called as the aircraft lift curve slope) can be determined from [79]:

$$C_{L\alpha} = C_{L\alpha_{wf}} + C_{L\alpha_h} \eta_h (S_h/S) (1 - d\epsilon/d\alpha) \quad (4.11)$$

$C_{L\alpha_{wf}}$ is the wing-fuselage lift curve slope, determined as [79]:

$$C_{L\alpha_{wf}} = K_{wf} C_{L\alpha_w} \quad (4.12)$$

where $C_{L\alpha_w}$ is the wing lift curve slope and is given by [79]:

$$C_{L\alpha_w} = 2\pi A / [2 + \{(A^2 \beta^2 / k^2)(1 + \tan^2 \Lambda_{c/2} / \beta^2) + 4\}^{1/2}] \quad (4.13)$$

$C_{L\alpha_h}$ is the horizontal tail lift curve slope. It can be calculated using the above equation with suitable substitution of horizontal tail parameters for the wing parameters. All other quantities in Eqs. 4.11-4.13 are defined in [79].

The derivative of the aerodynamic drag with respect to aircraft angle of attack can be computed as follows [79].

$$C_{D\alpha} = (\partial C_D / \partial C_L) C_{L\alpha} \quad (4.14)$$

The derivative of the aerodynamic pitching moment with respect to aircraft angle of attack can be calculated as follows [79].

$$C_{m_\alpha} = (\partial C_m / \partial C_L) C_{L_\alpha} \quad (4.15)$$

4.2.3 Angle of Sideslip Derivatives

The aircraft equations of motion contain the aerodynamic pitch velocity derivatives L_v , N_v , Y_v . They are derivatives of rolling moment, yawing moment and side force with respect to pitch velocity. If the angle of sideslip is very small then it is given by:

$$\beta = v/u \quad (4.16)$$

From the above equation:

$$\begin{aligned} L_\beta &= L_v u \\ N_\beta &= N_v u \\ Y_\beta &= Y_v u \end{aligned} \quad (4.17)$$

L_β , N_β and Y_β are calculated first to predict L_v , N_v and Y_v and given as [83],

$$\begin{aligned} L_\beta &= \frac{\bar{q}SbC_{l_\beta}}{I_x} \\ N_\beta &= \frac{\bar{q}SbC_{n_\beta}}{I_z} \\ Y_\beta &= \frac{\bar{q}SC_{y_\beta}}{m} \end{aligned} \quad (4.18)$$

The theoretical methods to predict the coefficients given in the above equations are described in this section.

The coefficient of the rolling moment derivative with respect to the sideslip, C_{l_β} (also called the dihedral effect) can be calculated from [79]:

$$C_{l_\beta} = C_{l_{\beta_{wf}}} + C_{l_{\beta_h}} + C_{l_{\beta_v}} \quad (4.19)$$

The wing-fuselage contribution is given by [79]:

$$\begin{aligned} C_{l_{\beta_{wf}}} &= \frac{180}{\pi} [C_{L_{wf}} \{ (C_{l_\beta}/C_L)_{\Lambda_c/2} (K_{M_\Lambda})(K_f) + (C_{l_\beta}/C_L)_A \} \\ &\quad + \Gamma \{ (C_{l_\beta}/\Gamma) K_{M_\Gamma} + (\Delta C_{l_\beta}/\Gamma) \} + (\Delta C_{l_\beta})_{z_w} \\ &\quad + (\epsilon_t \tan \Lambda_{c/4}) \{ (\Delta C_{l_\beta}) / (\epsilon_t \tan \Lambda_{c/4}) \}] \end{aligned} \quad (4.20)$$

The horizontal and vertical tail contributions are given by [79]:

$$C_{l_{\beta_h}} = (C_{l_{\beta_{hf}}})(S_h b_h / Sb)$$

$$C_{l_{\beta_v}} = (C_{y_{\beta_v}})\{(z_v \cos \alpha - l_v \sin \alpha)/b\} \quad (4.21)$$

The coefficient of the yawing moment derivative with respect to the sideslip, $C_{n_{\beta}}$ (also called static dihedral stability) is computed from [79]:

$$C_{n_{\beta}} = C_{n_{\beta_w}} + C_{n_{\beta_f}} + C_{n_{\beta_v}} \quad (4.22)$$

The wing, fuselage and vertical tail contributions are given in order as [79]:

$$\begin{aligned} C_{n_{\beta_w}} &= 0 \\ C_{n_{\beta_f}} &= \frac{-180}{\rho i} K_N K_{R1} (S_{f_s} b_f / S b) \\ C_{n_{\beta_v}} &= -(C_{y_{\beta_v}})\{(l_v \cos \alpha + z_v \sin \alpha)/b\} \end{aligned} \quad (4.23)$$

The coefficient of the side force derivative with respect to the sideslip, $C_{y_{\beta}}$ is calculated from [79]:

$$C_{y_{\beta}} = C_{y_{\beta_w}} + C_{y_{\beta_f}} + C_{y_{\beta_v}} \quad (4.24)$$

The wing, fuselage and vertical tail contributions are given in order as [79]:

$$\begin{aligned} C_{y_{\beta_w}} &= -0.00573(|\Gamma|) \\ C_{y_{\beta_f}} &= -2K_i(S_{cs}/S) \end{aligned}$$

$$C_{y\beta_v} = -k_v(C_{L\alpha_v})(1+d\sigma/d\beta)\eta_v(S_v/S) \quad (4.25)$$

4.2.4 Roll Rate Derivatives

The rolling moment with respect to the roll rate is [83],

$$L_p = \frac{\bar{q}Sb^2C_{l_p}}{2I_xu_0}$$

The coefficient of the rolling moment with respect to the roll rate C_{l_p} , also called the damping derivative, is found from [79]:

$$C_{l_p} = C_{l_{pw}} + C_{l_{ph}} + C_{l_{pv}} \quad (4.26)$$

The wing, horizontal and vertical tail contributions are given in order as [79]:

$$\begin{aligned} C_{l_{pw}} &= (\beta C_{l_p}/k)_{C_L=0}(k/\beta)\{(C_{L\alpha_w})_{C_L}/(C_{L\alpha_w})_{C_L=0}\} * \\ &\quad * \{(C_{l_p})_{\Gamma}/(C_{l_p})_{\Gamma=0}\} + (\Delta C_{l_p})_{drag} \\ C_{l_{ph}} &= 0.5(C_{l_p})_h(S_h/S)(b_h/b)^2 \\ C_{l_{pv}} &= 2(z_v/b)^2Y_{\beta_v} \end{aligned} \quad (4.27)$$

The derivative of the yawing moment with respect to the roll rate is [83],

$$N_p = \frac{\bar{q}Sb^2C_{n_p}}{2I_zu_0}$$

The derivative of the coefficient of the yawing moment with respect to the roll rate, C_{n_p} , is found from [79]:

$$C_{n_p} = C_{n_{pw}} + C_{n_{pv}} \quad (4.28)$$

The wing and vertical tail contributions are given in order as [79]:

$$\begin{aligned} C_{n_{pw}} &= \{(C_{n_p}/C_L)_{C_L=0}\}C_L + (C_{n_p}/\epsilon_t)\epsilon_t \\ &\quad + [\Delta C_{n_p}/\{(\alpha_{\delta_f})(\delta_f)\}](\alpha_{\delta_f})(\delta_f) \\ C_{n_{pv}} &= -(2/b^2)(l_v \cos\alpha + z_v \sin\alpha)(z_v \cos\alpha - l_v \sin\alpha - z_v)C_{y_{\beta_v}} \end{aligned} \quad (4.29)$$

The derivative of the side force with respect to the roll rate is [83],

$$Y_p = \frac{\bar{q}SbC_{n_p}}{2mu_0}$$

The derivative of the coefficient of the side force with respect to the roll rate C_{y_p} can be found from [79]:

$$C_{y_p} = 2(C_{y_{\beta_v}})\{(z_v \cos\alpha - l_v \sin\alpha)/b\} \quad (4.30)$$

4.2.5 Pitch Rate Derivatives

The pitching moment with respect to pitch rate derivative, also called pitch damping derivative is calculated from [79]:

$$C_{m_q} = C_{m_{q_w}} + C_{m_{q_h}} \quad (4.31)$$

The wing contribution is given by [79]:

$$C_{m_{q_w}} = C_{m_{q_w/at M=0}} \left\{ \frac{A^3 \tan^2 \Lambda_{c/4}}{AB + 6 \cos \Lambda_{c/4}} + \frac{3}{B} \right\} / \left\{ \frac{A^3 \tan^2 \Lambda_{c/4}}{A + 6 \cos \Lambda_{c/4}} + 3 \right\}$$

where $C_{m_{q_w/at M=0}} = -k_w C_{l_{\alpha_w}} \cos \Lambda_{c/4} \left[\frac{A \{ 2(x_w/\bar{c})^2 + 0.5(x_w/\bar{c}) \}}{(A + 2 \cos \Lambda_{c/4})} + \frac{A^3 \tan^2 \Lambda_{c/4}}{24(A + 6 \cos \Lambda_{c/4})} + \frac{1}{8} \right]$

The horizontal tail contribution is given by [79]:

$$C_{m_{q_h}} = -2(C_{L_{\alpha_h}}) \eta_h \bar{V}_h (\bar{x}_{ac_h} - \bar{x}_{cg}) \quad (4.32)$$

4.2.6 Yaw Rate Derivatives

The derivative of the rolling moment with respect to the yaw rate is [83],

$$L_r = \frac{\bar{q} S b^2 C_{l_r}}{2 I_x u_0}$$

The coefficient of the rolling moment with respect to the yaw rate C_{l_r} is determined from [79]:

$$C_{l_r} = C_{l_{rw}} + C_{l_{rv}} \quad (4.33)$$

The wing and vertical tail contributions are given in order as [79]:

$$\begin{aligned} C_{l_{rw}} &= (C_{L_w})(C_{l_r}/C_L)_{C_L=0} + (\Delta C_{l_r}/\Gamma)\Gamma + (\Delta C_{l_r}/\epsilon_t)\epsilon_t \\ &\quad + [\Delta C_{l_r}/\{(\alpha_{\delta_f})(\delta_f)\}](\alpha_{\delta_f})(\delta_f) \\ C_{l_{rv}} &= -(2/b^2)(l_v \cos\alpha + z_v \sin\alpha)(z_v \cos\alpha - l_v \sin\alpha)C_{y\beta_v} \end{aligned} \quad (4.34)$$

The yawing moment with respect to the yaw rate is [83],

$$N_r = \frac{\bar{q}Sb^2C_{n_r}}{2I_z u_0}$$

The coefficient of the yawing moment with respect to the yaw rate C_{n_r} , also called the yaw damping is found from [79]:

$$C_{n_r} = C_{n_{rw}} + C_{n_{rv}} \quad (4.35)$$

The wing and vertical tail contributions are given in order as [79]:

$$C_{n_{rw}} = (C_{n_r}/C_L^2)(C_{L_w})^2 + (C_{n_r}/C_{D_0})C_{D_{0w}}$$

$$C_{n_{r_v}} = (2/b^2)(l_v \cos \alpha + z_v \sin \alpha)^2 C_{y_{\beta_v}} \quad (4.36)$$

The side force with respect to the yaw rate is [83],

$$Y_r = \frac{\bar{q} S b C_{y_r}}{2 m u_0}$$

The coefficient of the side force with respect to the yaw rate C_{y_r} , is found from [79]:

$$C_{y_r} = -2(C_{y_{\beta_v}})\{(l_v \cos \alpha + z_v \sin \alpha)/b\} \quad (4.37)$$

4.3 Control Derivatives

The techniques to calculate the following control derivatives are addressed in this section:

1. Aileron control derivatives.
2. Elevator control derivatives.
3. Rudder control derivatives.

As it was stated before, only preliminary equations are addressed here. Complete analysis can be found from [79-83].

4.3.1 Aileron Control Derivatives

The rolling moment with respect to the aileron deflection is given as [83]

$$L_{\delta_a} = \frac{\bar{q}SbC_{l_{\delta_a}}}{I_x}$$

The coefficient of the rolling moment with respect to the aileron deflection, $C_{l_{\delta_a}}$, also called the roll control power, is calculated from [83]:

$$C_{l_{\delta_a}} = \frac{2C_{L_{\alpha_w}}\tau}{Sb} \int_{y_1}^{y_2} cy \, dy \quad (4.38)$$

The yawing moment with respect to the aileron deflection is given as [83]

$$N_{\delta_a} = \frac{\bar{q}SbC_{n_{\delta_a}}}{I_z}$$

The coefficient of the yawing moment with respect to the aileron deflection, $C_{n_{\delta_a}}$, also called the adverse aileron yaw, is predicted from [83]:

$$C_{n_{\delta_a}} = K_a C_{L_w} C_{l_{\delta_a}} \quad (4.39)$$

The side force with respect to the aileron deflection is given as [83]

$$Y_{\delta_a} = \frac{\bar{q}SC_{y_{\delta_a}}}{m}$$

The coefficient of the side force with respect to the aileron deflection, $C_{y_{\delta_a}}$ is negligible for most of the conventional aileron arrangements [80]:

$$C_{y_{\delta_a}} = 0 \quad (4.40)$$

4.3.2 Elevator Control Derivatives

The pitching moment with respect to elevator derivative, $C_{m_{\delta_e}}$, also called the elevator control power, can be found from [79]:

$$\begin{aligned} C_{m_{\delta_e}} &= (\alpha_{\delta_e})C_{m_{i_h}} \\ (\alpha_{\delta_e}) &= k_b \{c_{l_{\delta}} / (c_{l_{\delta}})_{theory}\} (c_{l_{\delta}})_{theory} (k' / c_{l_{\alpha_h}}) [(\alpha_{\delta})C_L / (\alpha_{\delta})c_l] \\ C_{m_{i_h}} &= -(C_{L_{\alpha_h}})\eta_h \bar{V}_h \end{aligned} \quad (4.41)$$

4.3.3 Rudder Control Derivatives

The rolling moment with respect to the rudder deflection is given as [83]

$$L_{\delta_r} = \frac{\bar{q}SbC_{l_{\delta_r}}}{I_x}$$

The coefficient of the rolling moment with respect to the aileron deflection, $C_{l_{\delta_r}}$, also called the roll control power, is calculated from [83]:

$$C_{l_{\delta_r}} = \{(z_v \cos \alpha - l_v \sin \alpha) / b\} C_{y_{\beta_v}} \quad (4.42)$$

The yawing moment with respect to the rudder deflection is given as [83]

$$N_{\delta_r} = \frac{\bar{q}SbC_{n_{\delta_r}}}{I_z}$$

The coefficient of the yawing moment with respect to the aileron deflection, $C_{n_{\delta_r}}$, also called the rudder control power, can be found from [79]:

$$C_{n_{\delta_r}} = -C_{y_{\beta_v}} \{(l_v \cos \alpha + z_v \sin \alpha) / b\} \quad (4.43)$$

The side force with respect to the rudder deflection is given as [83]

$$Y_{\delta_r} = \frac{\bar{q}SC_{y_{\delta_r}}}{m}$$

The coefficient of the side force with respect to the rudder deflection, $C_{y_{\delta_r}}$ is given as [79]:

$$C_{y_{\delta_r}} = (C_{L_{\alpha_v}})(k'K_b)\{(\alpha_{\delta})_{C_L}/(\alpha_{\delta})_{C_l}\}(\alpha_{\delta})_{C_l}(S_v/S) \quad (4.44)$$

CHAPTER 5

INVESTIGATED EXAMPLES OF SYSTEM IDENTIFICATION USING FLIGHT TEST DATA

Two separate experiments were performed to investigate the System Identification theory, which was detailed in Chapters 2 and 3. The filter error technique was used in both experiments.

Sections 5.1-5.2 provide experimental details, which were originally carried out at DFVLR, Institute of Flight Mechanics, Braunschweig, Federal Republic of Germany [68]. The first experiment of this thesis utilized the same flight parameters and flight test data, which were used in the original experiments. The results of the experiments and comparison with the earlier experiments [1, 68] are also presented. The second experiment was performed on a radio controlled, glow-powered aircraft trainer, the Hanger 9 Extra Easy. The flight test data were acquired at Auburn University, Auburn, AL, USA.

5.1 Estimation of Lateral Motion Derivatives using the Simulated Flight Data

This experiment was performed to estimate the lateral motion derivatives of an aircraft using a linear model and simulated aircraft response. The aircraft response was generated incorporating moderate to high level of turbulence [1]. Nominal values of the lateral motion aerodynamic derivatives used correspond to those obtained by parameter estimation from flight data recorded during the tests in a steady atmosphere with the research aircraft de Havilland DHC-2, shown in Fig. 5.1 [68]. Classical equations of aircraft motion including



Figure 5.1: The DLR *de Havilland DHC – II* Research Aircraft [84]

additional state and measurement noise were used to generate aircraft response time histories. The rudder and aileron excitations are applied in the experiment to provide realistic control inputs [68].

An aircraft model for lateral directional motion is given below, which was used to estimate the derivatives [68, 85, 86].

State equations:

$$\begin{aligned}
 \dot{p} &= L_p p + L_r r + L_{\delta_a} \delta_a + L_{\delta_r} \delta_r + L_v v + b_{x_{\dot{p}}} \\
 \dot{r} &= N_p p + N_r r + N_{\delta_a} \delta_a + N_{\delta_r} \delta_r + N_v v + b_{x_{\dot{r}}}
 \end{aligned} \tag{5.1}$$

Observation equations:

$$\begin{aligned}
\dot{p}_m &= L_p p + L_r r + L_{\delta_a} \delta_a + L_{\delta_r} \delta_r + L_v v + b_{y_{\dot{p}}} \\
\dot{r}_m &= N_p p + N_r r + N_{\delta_a} \delta_a + N_{\delta_r} \delta_r + N_v v + b_{y_{\dot{r}}} \\
\dot{a}_{y_m} &= Y_p p + Y_r r + Y_{\delta_a} \delta_a + Y_{\delta_r} \delta_r + Y_v v + b_{y_{a_y}} \\
p_m &= p + b_{y_p} \\
r_m &= r + b_{y_r}
\end{aligned} \tag{5.2}$$

The unknown parameter vector Φ for the considered model has dimensional derivatives and bias terms. It is given as [68]:

$$\begin{aligned}
\Phi^T &= [L_p \ L_r \ L_{\delta_a} \ L_{\delta_r} \ L_v \ N_p \ N_r \ N_{\delta_a} \ N_{\delta_r} \ N_v \ Y_p \ Y_r \\
&\quad Y_{\delta_a} \ Y_{\delta_r} \ Y_v \ b_{x_{\dot{p}}} \ b_{x_{\dot{r}}} \ b_{y_{\dot{p}}} \ b_{y_{\dot{r}}} \ b_{y_{a_y}} \ b_{y_p} \ b_{y_r} \ f_{pp} \ f_{rr}]
\end{aligned} \tag{5.3}$$

Each element of the parameter vector Φ is defined in the above equations except f_{pp} and f_{rr} . They form diagonal process noise distribution matrix F. The initial values were kept the same as they were in the original experiment [68].

5.1.1 Comparison of the Results with the Original Experiment

The estimated results for the lateral motion derivatives, applying the system identification techniques discussed in Chapters 2 and 3, are summarized in Table 5.1. Initial and nominal values of the derivatives [1] are also given in the table. The results obtained from

Table 5.1: Estimated dimensional derivatives of lateral motion of aircraft

Parameter	Initial Value	Nominal Value	Estimated Value from this experiment	Estimated Value from the original experiment [68]
L_p	-6.700	-5.820	-5.818 (0.33)	-5.718 (6.6)
L_r	1.830	1.782	1.781 (0.42)	1.720 (9.1)
L_{δ_a}	-18.300	-16.434	-16.431 (0.53)	-14.925 (11.1)
L_{δ_r}	0.430	0.434	0.444 (4.80)	0.200 (216)
L_v	-0.114	-0.097	-0.097 (0.59)	-0.0883 (12.8)
N_p	-0.906	-0.665	-0.667 (1.23)	-0.621 (9.4)
N_r	-0.665	-0.712	-0.711 (0.45)	-0.722 (3.4)
N_{δ_a}	-0.660	-0.428	-0.427 (8.61)	-0.427 (58.9)
N_{δ_r}	-2.820	-2.824	-2.825 (0.32)	-2.828 (2.4)
N_v	0.0069	0.0084	0.0084 (2.88)	0.0092 (19.0)
Y_p	-0.640	-0.278	-0.272 (8.79)	-0.297 (27.7)
Y_r	1.300	1.410	1.408 (0.66)	1.415 (2.5)
Y_{δ_a}	-1.400	-0.447	-0.449 (23.91)	-0.514 (72.9)
Y_{δ_r}	2.790	2.657	2.659 (1.02)	2.688 (3.7)
Y_v	-0.193	-0.180	-0.180 (0.39)	-0.180 (1.5)
Iterations			6	10
Cost Function			6.406×10^{-32}	2.146×10^{-12}

The values in parenthesis indicate percent standard deviation

this experiment are compared with the results of the original experiment [68]. The comparison of the estimated values shows that the results from the present work are as close to the nominal values as the results from the original experiment. The filter error method converged within 6 iterations. Neither singularity nor convergence problems were found to occur.

After utilizing the statistical estimation techniques, the first and the most question is asked about the statistical accuracy of the estimates which are obtained in these experiments. The maximum likelihood estimator is asymptotically more efficient [1] in the sense of achieving smaller standard deviations which can be computed by $\sigma_{\Phi_i} = P1^{-1}$. The

asymptotic efficiency is an important property with practical importance. It implies that the maximum likelihood estimator makes efficient use of the available data and that the smaller standard deviation indicates theoretically maximum achievable accuracy of the estimates [1]. Tables 5.1-5.5 indicate that the standard deviation of all estimated derivatives are smaller, which means the estimates are very accurate.

5.1.2 Responses and Results

The comparison of the estimated model response with the measured data and the time history plots of the control inputs are shown in Fig. 5.2. As it was stated before, the control inputs and flight data used in this experiment are same as the original experiment [68]. The estimated data are shown in green while the measured data are shown as blue. Fig. 5.3 shows the convergence plots of the estimated parameters, which suggest all parameters are converging to a specific constant value within 6 iterations.

Reduction of the cost function appears in Fig. 5.4, which shows how rapidly the cost function reduces. This is due to the modified Newton-Raphson technique, which finds zero for the gradient of the cost function at the local minimum point. Also, the theoretically predicted parameters are very close to the estimated parameters using the algorithm. This is the prime reason the cost function is very small. Recalling the formulations for process noise discussed in Section 3.1.2, the combined formulation was used in this experiment. From Table 5.1 and Figs. 5.2-5.4 the following points are observed.

1. The measured response and the estimated response are in agreement with each other.

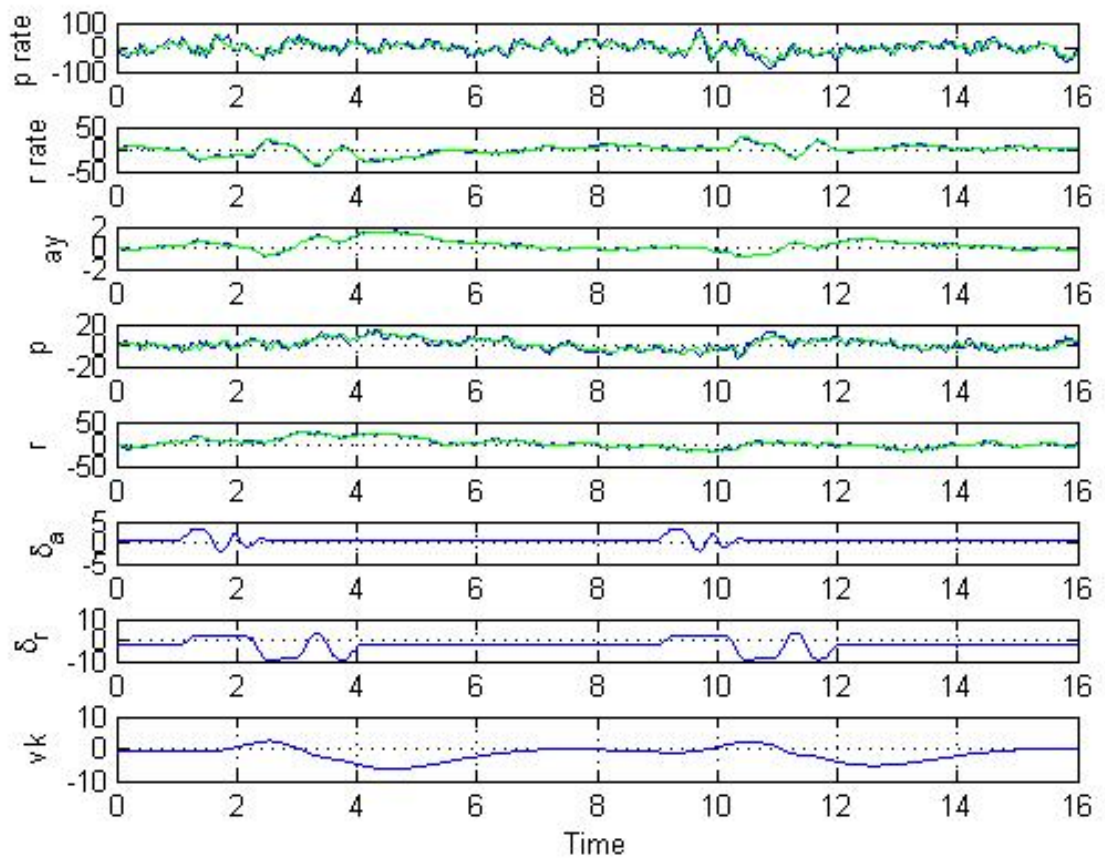


Figure 5.2: Comparison of Estimated (green) and Measured (blue) Responses for the Lateral Directional Motion of Aircraft

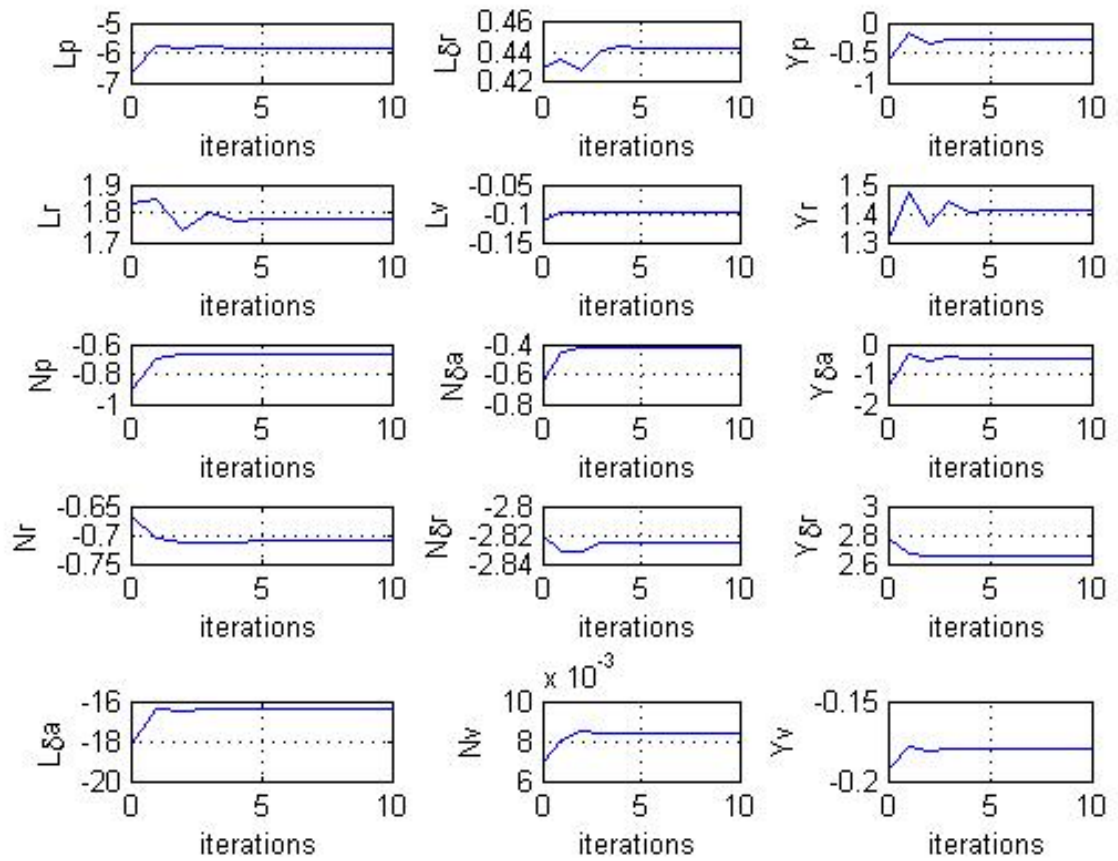


Figure 5.3: Convergence Plots of Dimensional Derivatives for Lateral Directional Motion of Aircraft

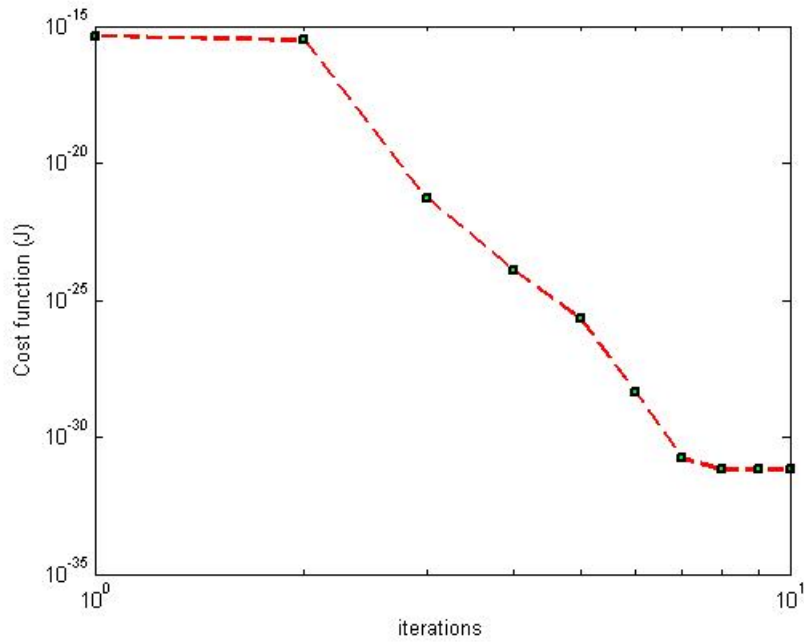


Figure 5.4: Cost Function Reduction for Lateral Directional Motion of Aircraft

2. All derivatives converged smoothly within only 4 iterations in comparison with the original experiment [68], where they converged in 10 iterations. Also, the estimated derivatives of this experiment are very close to the nominal values in comparison with the original one [68].
3. The cost function was reduced to a very low value, which was approximately zero.

The observations showed the combined formulation works well with process and measurement noise.



Figure 5.5: The DLR *HFB* – 320 Research Aircraft [87]

5.2 Estimation of Longitudinal Motion Derivatives of HFB-320 Aircraft

This experiment was performed to estimate the non dimensional derivatives of another aircraft. A non-linear model of a fixed wing research aircraft, the HFB-320, shown in Fig. 5.5, was used and the drag, lift and pitching moment coefficients of this research aircraft were estimated [87]. The longitudinal motion of the aircraft was excited through flight tests [88]. A multi-step elevator input was used in the flight test, which resulted in a short period motion, as well as a pulse input, that lead to a phugoid motion [89]. The inputs are shown in Fig. 5.8.

A non-linear model of longitudinal motion of aircraft was utilized in the experiment because the non-linear model was found to provide excellent estimation results [88-90]. The postulated non-linear model to estimate the non-dimensional aerodynamic derivatives is

described below [1]. This model is in terms of non-dimensional derivatives (the drag, lift and pitching moment coefficients), which are functions of variables in the wind axes (V , α , q , etc.) [68].

State equations:

$$\begin{aligned}
\dot{V} &= -\frac{\bar{q}S}{m}C_D + g\sin(\alpha - \theta) + \frac{F_e}{m}\sin(\alpha + \sigma_T) \\
\dot{\alpha} &= -\frac{\bar{q}S}{mV}C_L + q + \frac{g}{V}\cos(\alpha - \theta) - \frac{F_e}{mV}\sin(\alpha + \sigma_T) \\
\dot{\theta} &= q \\
\dot{q} &= \frac{\bar{q}S\bar{c}}{I_y}C_m + \frac{F_e}{I_y}(l_{tx}\sin\alpha_T + l_{tz}\cos\sigma_T)
\end{aligned} \tag{5.4}$$

where the lift, drag and pitching moment coefficients are given as:

$$\begin{aligned}
C_D &= C_{D0} + C_{DV}\frac{V}{V_0} + C_{D\alpha}\alpha \\
C_L &= C_{L0} + C_{LV}\frac{V}{V_0} + C_{L\alpha}\alpha \\
C_m &= C_{m0} + C_{mV}\frac{V}{V_0} + C_{m\alpha}\alpha + C_{mq}\frac{q\bar{c}}{2V_0} + C_{m\delta_e}\delta_e
\end{aligned} \tag{5.5}$$

Observation equations:

$$V_m = V$$

$$\alpha_m = \alpha$$

$$\theta_m = \theta$$

Table 5.2: Estimated non-dimensional derivatives of longitudinal motion of aircraft

Parameter	Initial Value	Estimated Value from this experiment	Estimated Value from the original experiment [68]
C_{D_0}	0.0057	0.12374 (9.37)	0.1227 (2.4)
C_{D_V}	0.0077	-0.0654 (9.88)	-0.0645 (3.9)
C_{D_α}	0.6742	0.31952 (11.41)	0.3201 (2.2)
C_{L_0}	-0.3183	-0.09548 (13.18)	-0.0952 (20)
C_{L_V}	0.2603	0.15600 (8.78)	0.1500 (10)
C_{L_α}	5.3758	4.27838 (4.92)	4.3386 (1.1)
C_{m_0}	0.0498	0.09319 (11.47)	0.1141 (3.3)
C_{m_V}	0.0189	0.01488 (14.07)	0.0022 (152)
C_{m_α}	-0.4986	-0.89514 (3.24)	-0.9705 (1.1)
C_{m_q}	-25.844	-38.24428 (5.93)	-34.021 (2.3)
$C_{m_{\delta_e}}$	-0.9907	-1.49040 (3.66)	-1.5228 (1.3)
V_0	104.67	104.36	106.024
α_0	0.1971	0.1085	0.1117
θ_0	0.1317	0.1543	0.1049
q_0	0.0469	-0.00468	-0.00333
Iterations		6	12
Cost Function		8.514×10^{-30}	3.1256×10^{-31}

Values in parenthesis indicate percent standard deviation

$$\begin{aligned}
 q_m &= q \\
 \dot{q}_m &= \frac{\bar{q}S\bar{c}}{I_y}C_m + \frac{F_e}{I_y}(l_{tx}\sin\alpha_T + l_{tz}\cos\sigma_T) \\
 a_{xm} &= \frac{\bar{q}S}{m}C_X + \frac{F_e}{m}\cos\sigma_T \\
 a_{zm} &= \frac{\bar{q}S}{m}C_Z - \frac{F_e}{m}\sin\sigma_T
 \end{aligned} \tag{5.6}$$

where the longitudinal and vertical force coefficients C_X and C_Z are modeled as

$$\begin{aligned}
 C_X &= C_L\sin\alpha - C_D\cos\alpha \\
 C_Z &= C_L\cos\alpha - C_D\sin\alpha
 \end{aligned} \tag{5.7}$$

The above mentioned non-linear aircraft model of Eqs. 5.4-5.6, contains non-linearities due to trigonometric terms, \bar{q} and also on account of the transformation in Eq. 5.7.

The unknown parameter vector Φ for the considered model has non-dimensional derivatives, and is given below as [1]:

$$\Phi^T = [C_{D0} \ C_{DV} \ C_{D\alpha} \ C_{L0} \ C_{LV} \ C_{L\alpha} \ C_{m0} \ C_{mV} \ C_{m\alpha} \ C_{mq} \ C_{m\delta_e}] \quad (5.8)$$

5.2.1 Comparison of the Results with the Original Experiment

The estimated results from the longitudinal motion derivatives, applying the system identification technique discussed in Chapters 2 and 3, are summarized in the Table 5.2. Initial values of the non-dimensional derivatives [1] are also given in the table. The results obtained from this experiment are compared with the results of the original experiment [68]. Neither singularity nor convergence problems were found to occur in this experiment.

5.2.2 Responses and Results

The comparison of the estimated model response with the measured data and the time history plots of the control inputs are shown in Fig. 5.6. The estimated data are shown in green while the measured data are shown in blue. Fig. 5.7 shows the convergence plots of the estimated parameters, which suggest all derivatives converged smoothly within only 4 iterations in comparison with the original experiment [68], where they converged in 12

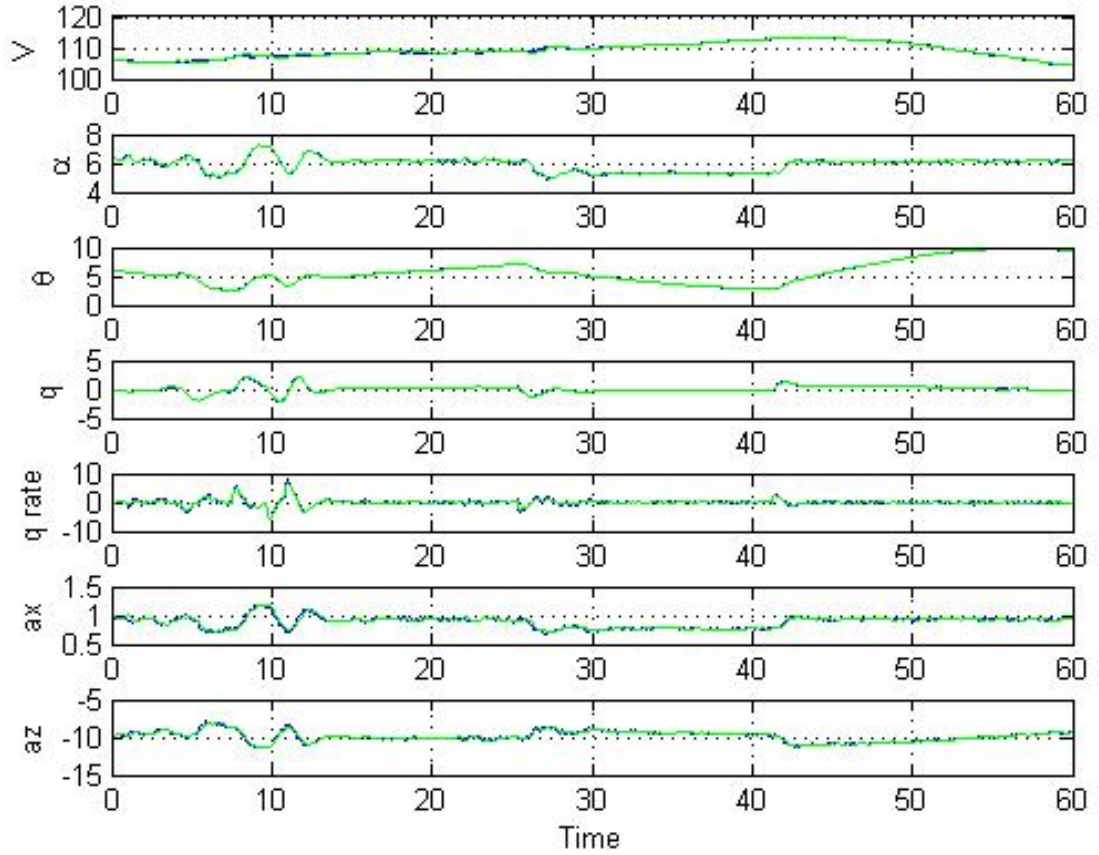


Figure 5.6: Comparison of Estimated (green) and Measured (blue) Responses for the Longitudinal Directional Motion of Aircraft

iterations. Also, the estimated derivatives of this experiment are very close to the nominal values [68].

Reduction of the cost function appears in Fig. 5.9, which shows how rapidly the cost function was reduced.

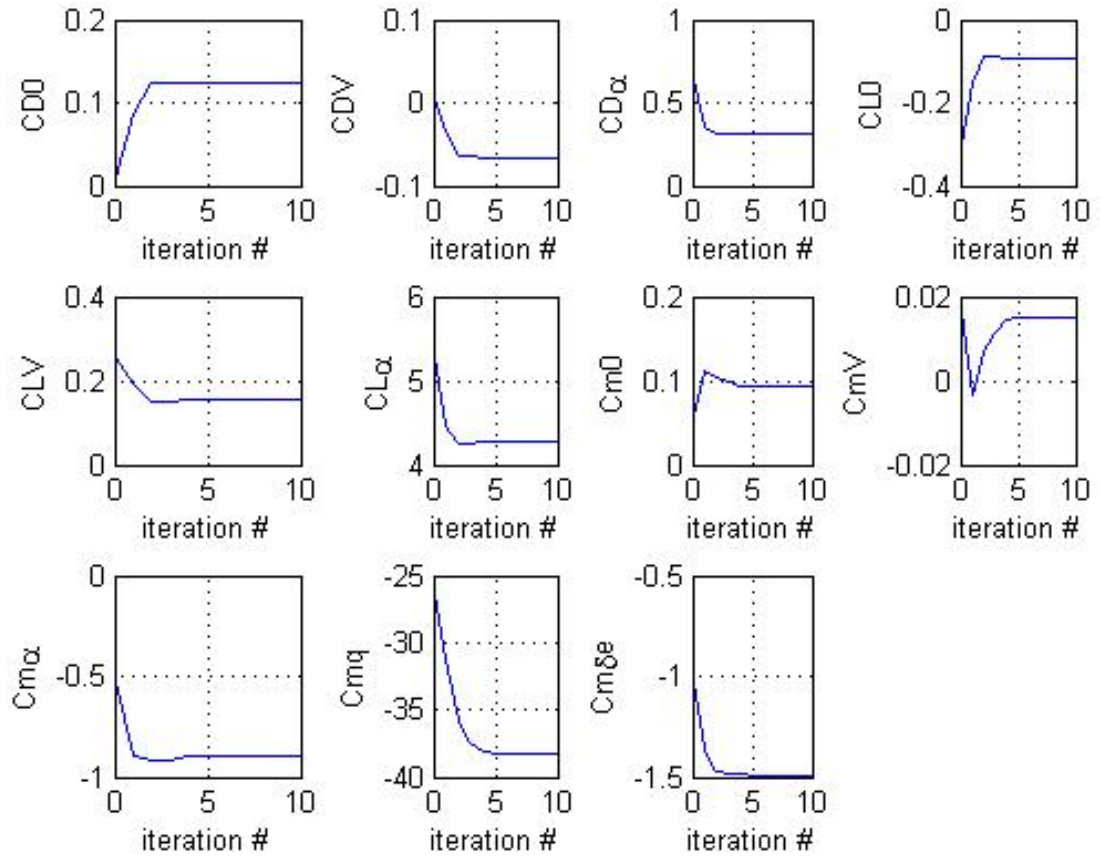


Figure 5.7: Convergence Plots of Non-Dimensional Derivatives for Longitudinal Directional Motion of Aircraft

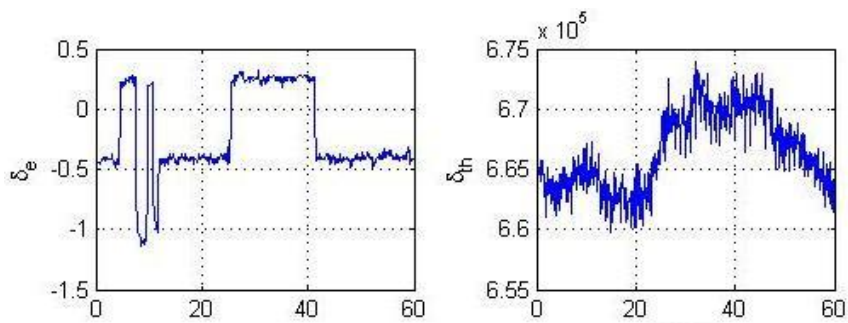


Figure 5.8: Inputs for Longitudinal Motion

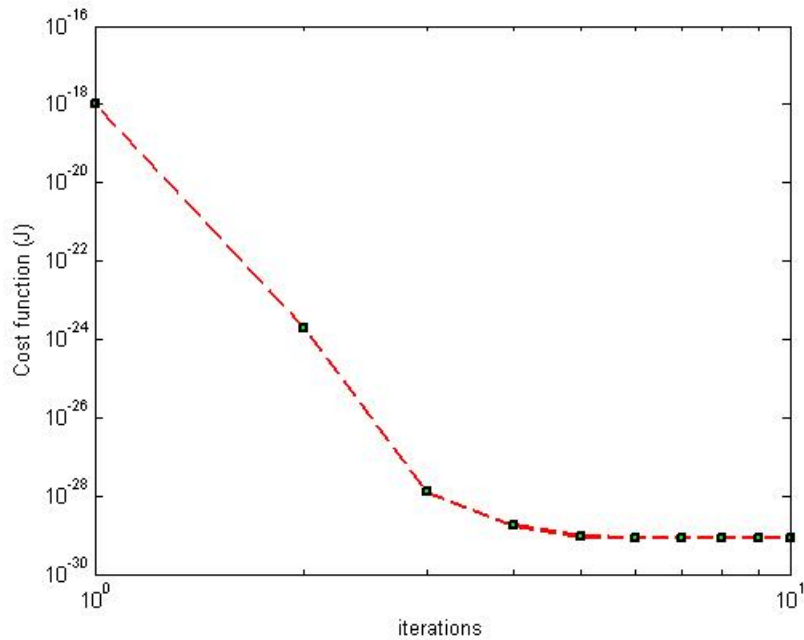


Figure 5.9: Cost Function Reduction for Longitudinal Motion

5.3 System Identification Applied to Model Aircraft Trainer

The experiments discussed in sections 5.1-5.2 were successfully completed. As a final part of the exercise, the system identification technique was applied to model aircraft trainer. The filter error technique for linear and nonlinear systems discussed in Chapter 3 were applied here, as well as the modified Newton-Raphson algorithm to reduce the cost function. The experiment and results are discussed in the following subsections.

5.3.1 The Investigated Aircraft Trainer - Hanger 9 Extra Easy

An unmanned aerial aircraft trainer, Hanger 9 Extra Easy which is made by Hobby Outlet (shown in Fig. 5.10), was investigated in the third experiment. The Hanger 9 Extra



Figure 5.10: Aircraft Trainer - Hanger 9 Extra Easy [91]

Easy is a radio controlled glow powered aircraft. Both, lateral and longitudinal motion derivatives were estimated for this aircraft. For lateral directional motion, a linear model was used and the state and observation equations of Eqs. 5.1-5.2 were utilized. The unknown parameter vector Φ of Eq. 5.3 was estimated. For longitudinal directional motion, a non-linear model was used and the state and observation equations of Eqs. 5.4-5.7 were utilized. The unknown parameter vector Φ of Eq. 5.8 was estimated. The aerodynamic, geometric and mass details of the trainer aircraft [91] are given in the following Table 5.3. Geometric details were provided by the manufacturer and the remaining details were measured from the aircraft.

5.3.2 Responses and Results

The stability and control derivatives of the aircraft trainer, given in Eq. 5.3 and Eq. 5.8 were estimated in this part of experiment. The initial value of each derivative

Table 5.3: Aerodynamic, geometric and mass data for the aircraft trainer

Parameter Detail	Data	Parameter Detail	Data
Wing Area, S, ft^2	4.8472	Horizontal tail Area, S_t, ft^2	1.0938
Mach number, M	0.2	Vertical tail Area, S_t, ft^2	0.9375
Aircraft side Area, S_{side}, ft^2	1.4637	Aircraft planform Area, S_{plf}, ft^2	1.0664
Aircraft cross sectional Area, S_{cs}, ft^2	0.167	Aircraft wetted Area, S_{wet}, ft^2	4.3005
Wing Span, ft	5.167	Horizontal tail Span, b_t, ft	
Wing mean aerodynamic chord, \bar{c}, ft	0.9375	Horizontal tail mean aerodynamic chord, \bar{c}_t, ft	0.6035
Wing aspect ratio, A	5.5072	Horizontal tail aspect ratio, A_t	0.9142
Location of the wing 1/4 root chord on the fuselage, fraction of the fuselage length, l_f	0.2614	Aircraft center of arm, l_t , gravity, X_{cg} , Back from the leading edge of the wing, <i>percent</i>	0.2919
Wing lift curve slop $C_{L_{\alpha_w}}, rad^{-1}$	4.8	Horizontal tail lift curve slope, $C_{L_{\alpha_t}}, rad^{-1}$	3.5
Span efficiency factor, e	0.75	Ambient air density, $\rho, slug/ft^3$	0.002377
Fuselage length, l_f, ft	4.2917	Fuselage width, w_f, ft	0.2817
Horizontal distance between vertical tail a.c. and aircraft wing a.c., l_p, ft	2.33	Horizontal distance between vertical tail a.c. and aircraft c.g. l_v, ft	2.52
Vertical distance between vertical tail a.c. and aircraft wing a.c., z_p, ft	0.145	Vertical distance between vertical tail a.c. and aircraft c.g., z_v, ft	0.4292
Aircraft weight, W, lbs	8.64	Aircraft speed $V_0, ft/s$	58.67
Center of gravity location, percent of \bar{c} , measured from leading edge	31	Compressible Sweep Correction Factor, B	1
Position of a.c. on wing m.g.c., X_{ac}, ft	0.1781	Position of horizontal tail a.c. on wing m.g.c., X_{ach}, ft	2.7552
Aircraft mass moment of inertia, $I_{yy}, slug - ft^2$	0.2712	Sweep angle at leading edge, Λ_{LE}, deg	0
Angle of attack, α, deg	5	sideslip angle, β, deg	0
Dynamic pressure, $\bar{q}, lb/ft^2$	4.1	Taper ratio, λ	1
Wing dihedral angle, Γ, deg	3	Wing twist angle, ϵ_t, deg	0
Semi chord Sweep angle, $\Lambda_{c/2}$	0	Quarter chord Sweep angle, $\Lambda_{c/2}$	0
Coefficient of viscosity of air, $\mu, slug/ft^3, deg$	0.374e-6	Thickness ratio at mean geometric chord, $t/c, deg$	0.12
Reynolds number of wing, $R_{N_{wing}}$	0.807e6	Reynolds number of fuselage, $R_{N_{fuse}}$	3.7e6

Table 5.4: Comparison between the predicted values and the estimated values of the dimensional derivatives for the lateral motion of the aircraft trainer

Parameter	Predicted Values	Estimated Values
L_p	-8.9091	-9.5691 (5.68)
L_r	3.8293	—————
L_{δ_a}	25.3741	30.6561 (5.28)
L_{δ_r}	-3.8108	—————
L_v	0.6043	2.6734 (8.65)
N_p	1.0091	1.3091 (8.12)
N_r	-0.4112	—————
N_{δ_a}	-2.0027	-2.9756 (11.88)
N_{δ_r}	-5.7743	—————
N_v	0.1953	0.3232 (18.9)
Y_p	-0.1964	-0.2967 (6.11)
Y_r	-0.0564	—————
Y_{δ_a}	0.0000	—————
Y_{δ_r}	-0.3438	—————
Y_v	0.5251	0.1203 (10.09)

Values in parenthesis indicate percent standard deviation

was determined using the techniques detailed in Chapter 4. The comparison between the predicted initial values and the estimated values, of the lateral dimensional derivatives are summarized in the Tables 5.4-5.5. The comparison between the predicted values and the estimated values of the longitudinal non-dimensional derivatives are summarized in the Table 5.6. The figures showing responses use the metric units for the length related parameters and the degree units for the angle related parameters.

For the lateral motion of the aircraft trainer, two different data sections from the same flight data were analyzed. The aileron and the rudder control inputs were applied simultaneously in both the data sections. First consider that data section in which the aileron control input was applied. While analyzing this particular data section, the derivatives with respect to the yaw velocity and the derivatives with respect to the rudder deflection, were

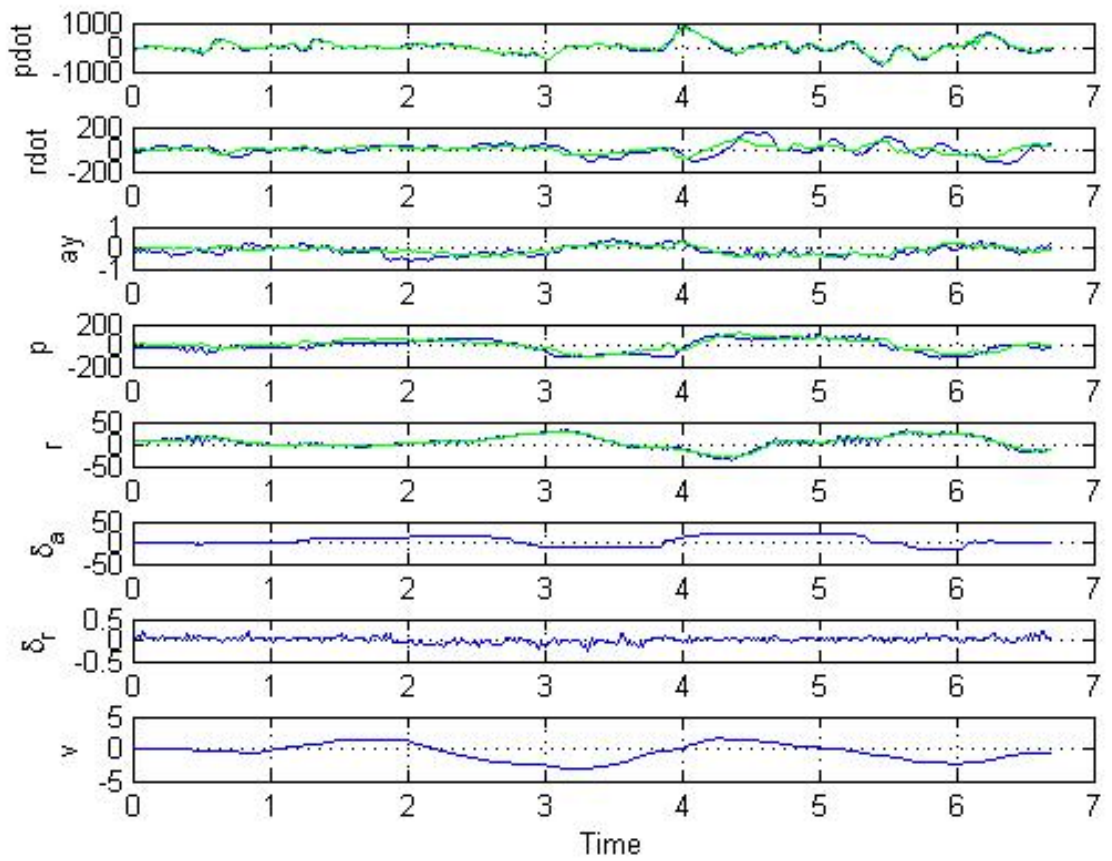


Figure 5.11: Comparison of Estimated (green) and Measured (blue) Responses for the Lateral Directional Motion of Aircraft

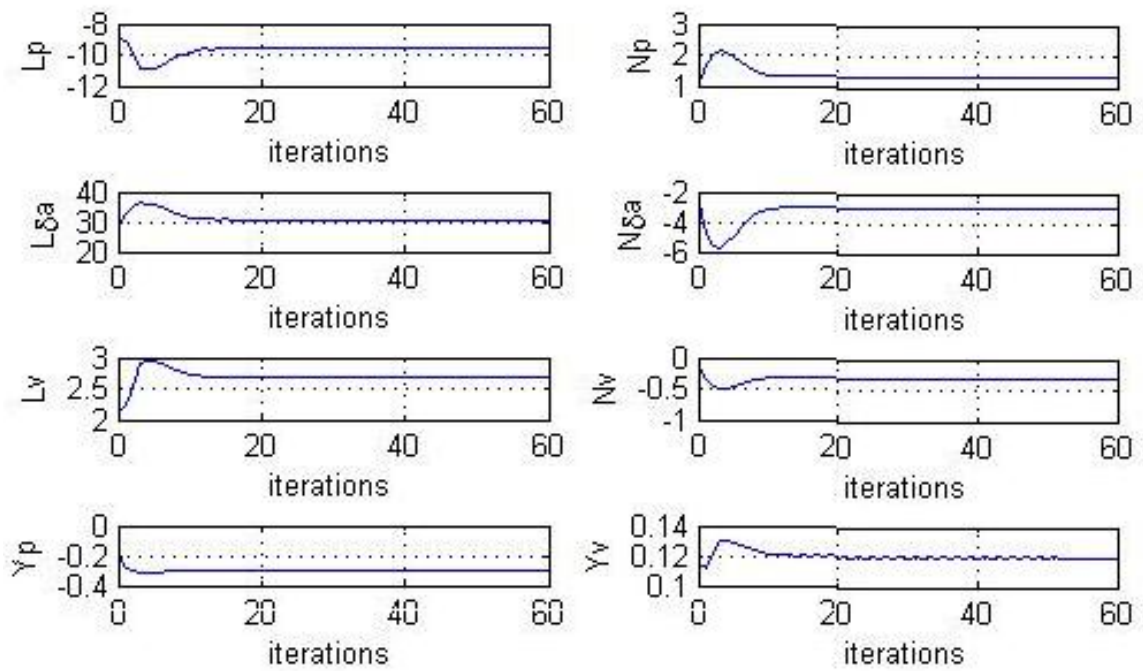


Figure 5.12: Convergence Plots of Dimensional Derivatives for Lateral Directional Motion of Aircraft

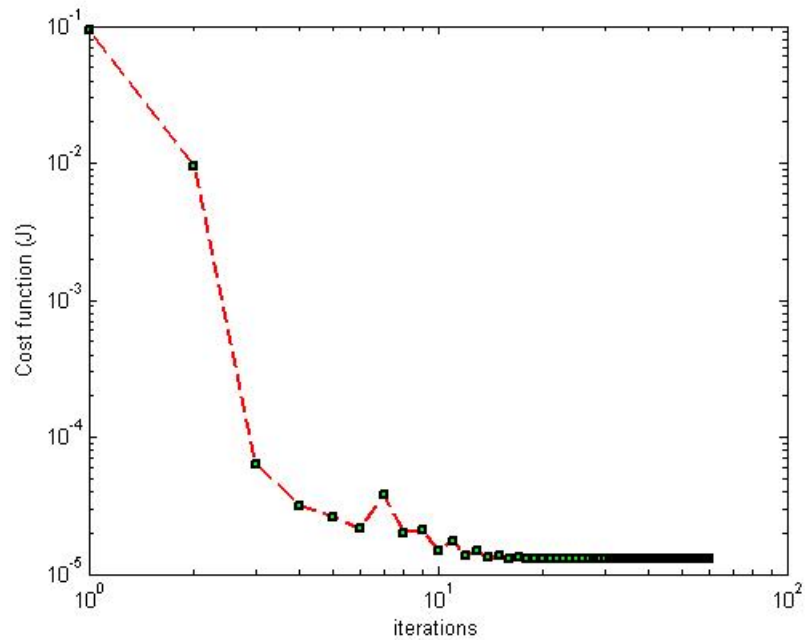


Figure 5.13: Cost Function Reduction for Lateral Directional Motion of Aircraft

kept constant. Table 5.4 shows comparison between the predicted values and the estimated values of the accounted derivatives. The predicted and estimated values are very close as that can be concluded from the Table 5.4.

The Fig. 5.11 shows comparison between the estimated and the measured parameters. It also shows the inputs utilized for this experiment. The estimated parameters are very close to the measured parameters. Fig. 5.12 shows the convergence of the derivatives.

Now, consider that data section in which the rudder control input was applied. While analyzing this data section the derivatives with respect to the roll velocity and the derivatives with respect to the aileron deflection, were kept constant. Table 5.5 shows comparison

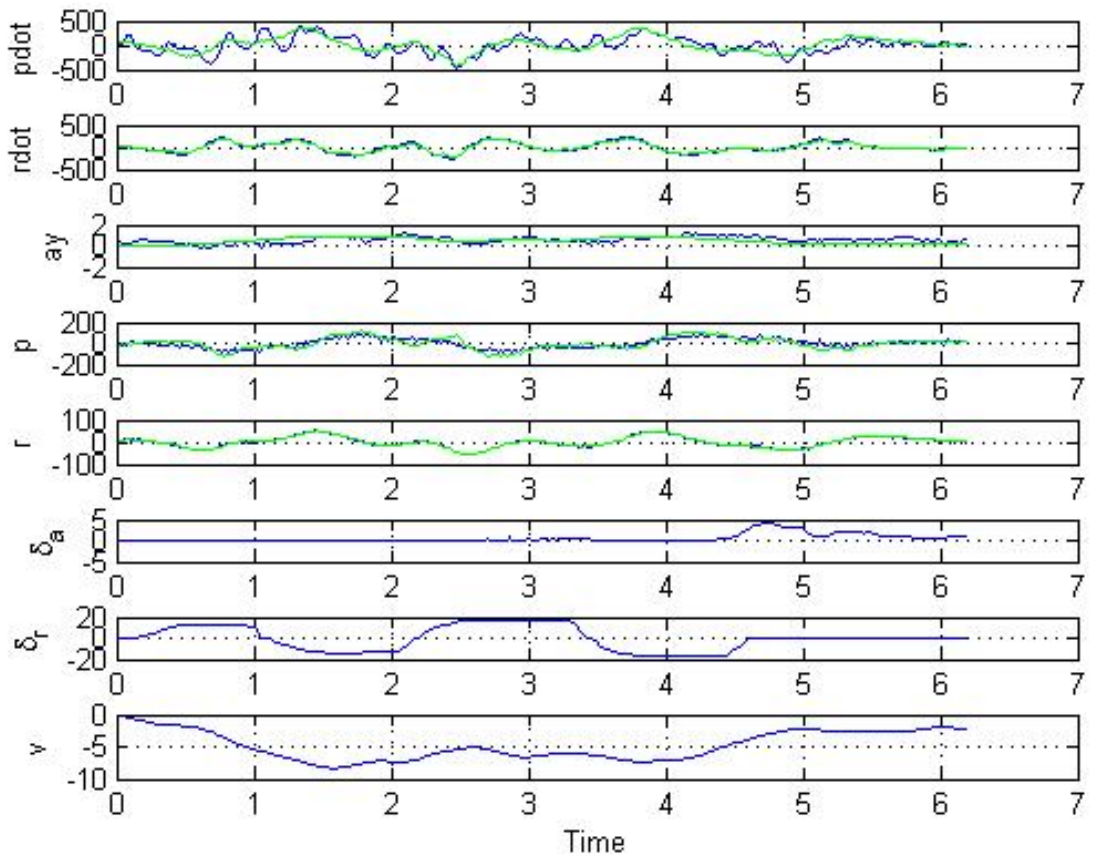


Figure 5.14: Comparison of Estimated (green) and Measured (blue) Responses for the Lateral Directional Motion of Aircraft

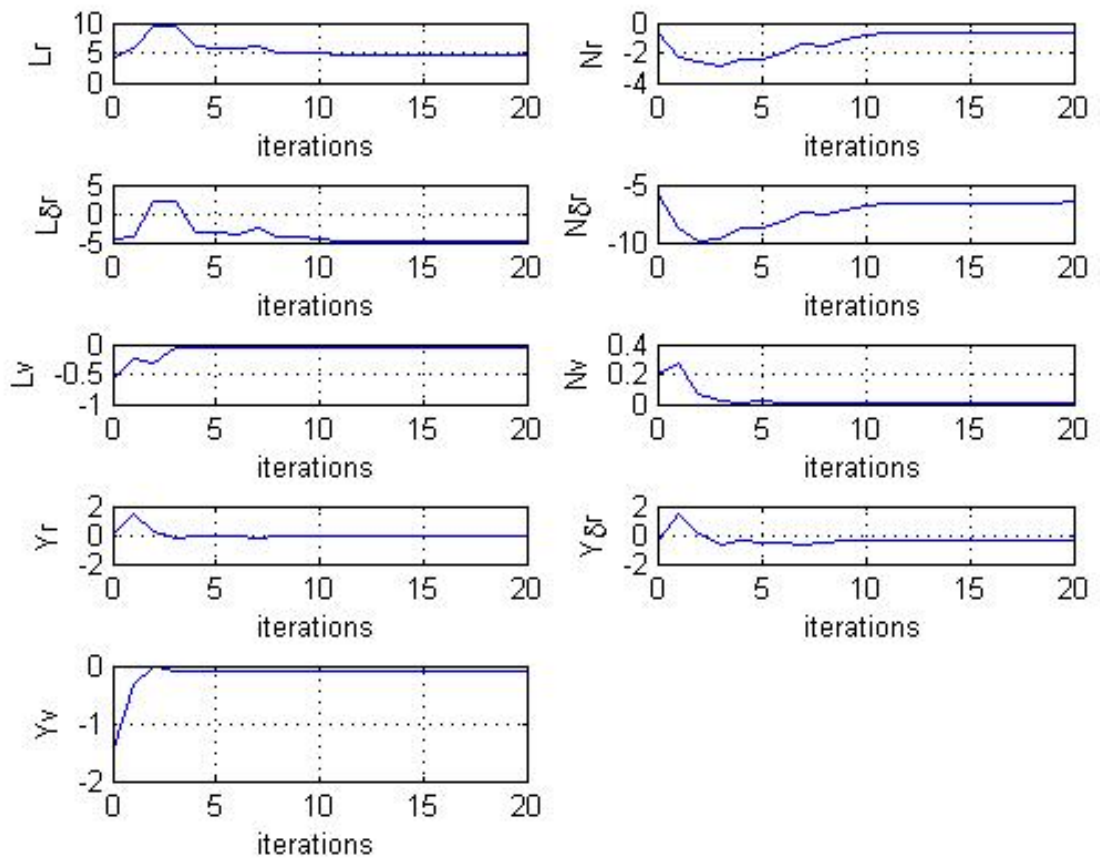


Figure 5.15: Convergence Plots of Dimensional Derivatives for Lateral Directional Motion of Aircraft

Table 5.5: Comparison between the predicted values and the estimated values of the dimensional derivatives for the lateral motion of the aircraft trainer

Parameter	Predicted Values	Estimated Values
L_p	-8.9091	————
L_r	3.8293	4.5890 (8.46)
L_{δ_a}	25.3741	————
L_{δ_r}	-3.8108	-4.7749 (19.71)
L_v	0.6043	-0.0435 (9.43)
N_p	1.0091	————
N_r	-0.4112	-0.6200 (17.31)
N_{δ_a}	-2.0027	————
N_{δ_r}	-5.7743	-6.5220 (7.3)
N_v	0.1953	0.0135 (25.36)
Y_p	-0.1964	————
Y_r	-0.0564	-0.0614 (27.9)
Y_{δ_a}	0.0000	————
Y_{δ_r}	-0.3438	-0.4526 (25.26)
Y_v	0.5251	-0.1016 (3.39)

Values in parenthesis indicate percent standard deviation

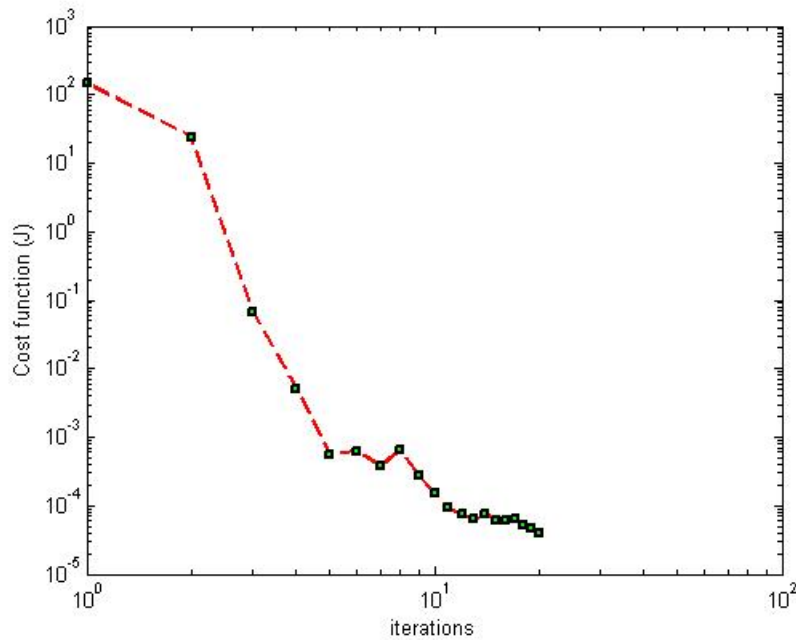


Figure 5.16: Cost Function Reduction for Lateral Directional Motion of Aircraft

Table 5.6: Comparison between the predicted values and the estimated values of the non-dimensional derivatives for the longitudinal motion of aircraft trainer

Parameter	Predicted Values	Estimated Values
C_{D_0}	0.0232	————
C_{D_V}	0.0000	————
C_{D_α}	0.0021	0.0893 (9.25)
C_{L_0}	0.2243	-0.0202 (4.55)
C_{L_V}	0.0000	————
C_{L_α}	0.1543	0.1274 (7.38)
C_{m_0}	0.0106	-0.0194 (19.72)
C_{m_V}	0.0000	————
C_{m_α}	-0.4286	-1.2563 (10.97)
C_{m_q}	-23.7257	-30.2730 (6.36)
$C_{m_{\delta_e}}$	2.9213	3.3677 (5.36)

Values in parenthesis indicate percent standard deviation

between the predicted values and the estimated values of the accounted derivatives. The predicted and estimated values are very close as that can be concluded from the Table 5.5.

The Fig. 5.14 shows comparison between the estimated and the measured parameters. It also shows the inputs utilized for this experiment. The estimated parameters are very close to the measured parameters. Fig. 5.15 shows the convergence of the derivatives.

To estimate the longitudinal motion of the aircraft trainer, consider that data section where the elevator control input was given. The aircraft drag due to zero lift was found unobservable in this experiment. Hence it was not estimated and its predicted value was used as a constant value. Table 5.6 shows comparison between the predicted values and the estimated values of the accounted derivatives. From Table 5.6 it can be said that the predicted and the estimated values are very close.

The Fig. 5.17 shows comparison between the estimated and the measured parameters. Fig. 5.19 shows the inputs utilized for this experiment.

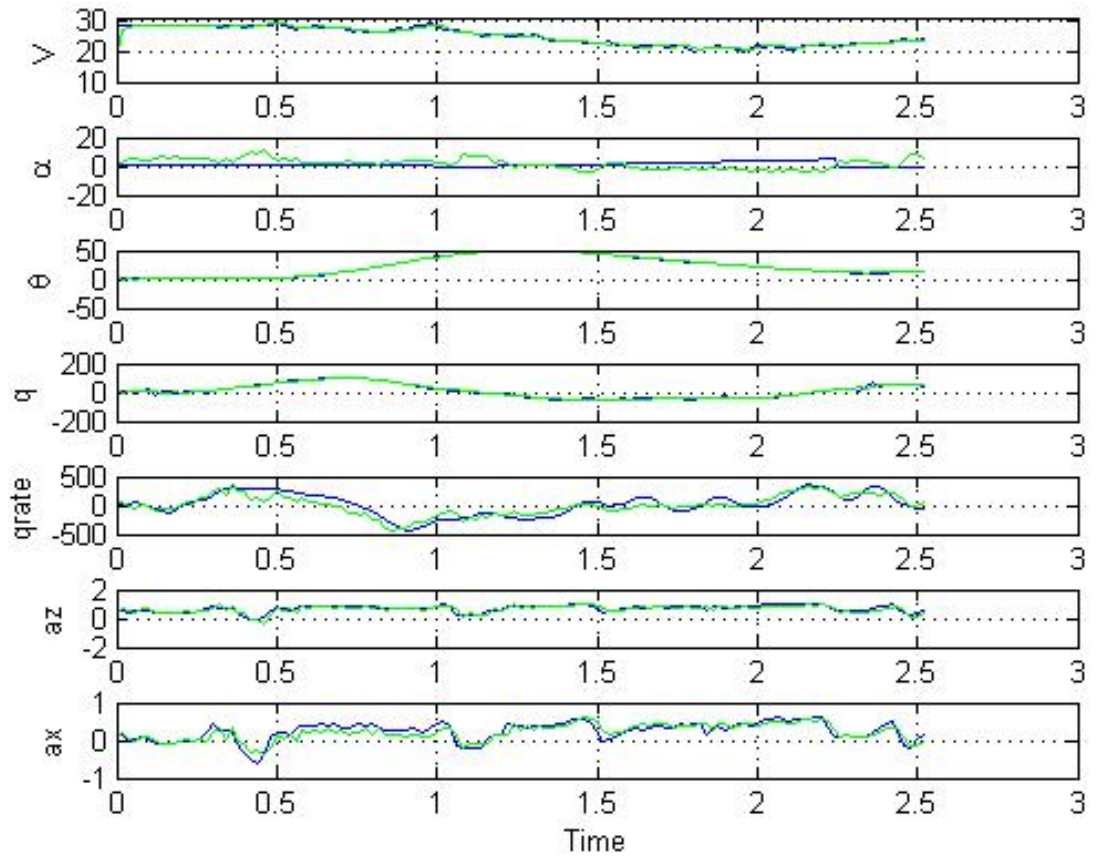


Figure 5.17: Comparison of Estimated (green) and Measured (blue) Responses for the Longitudinal Directional Motion of Aircraft

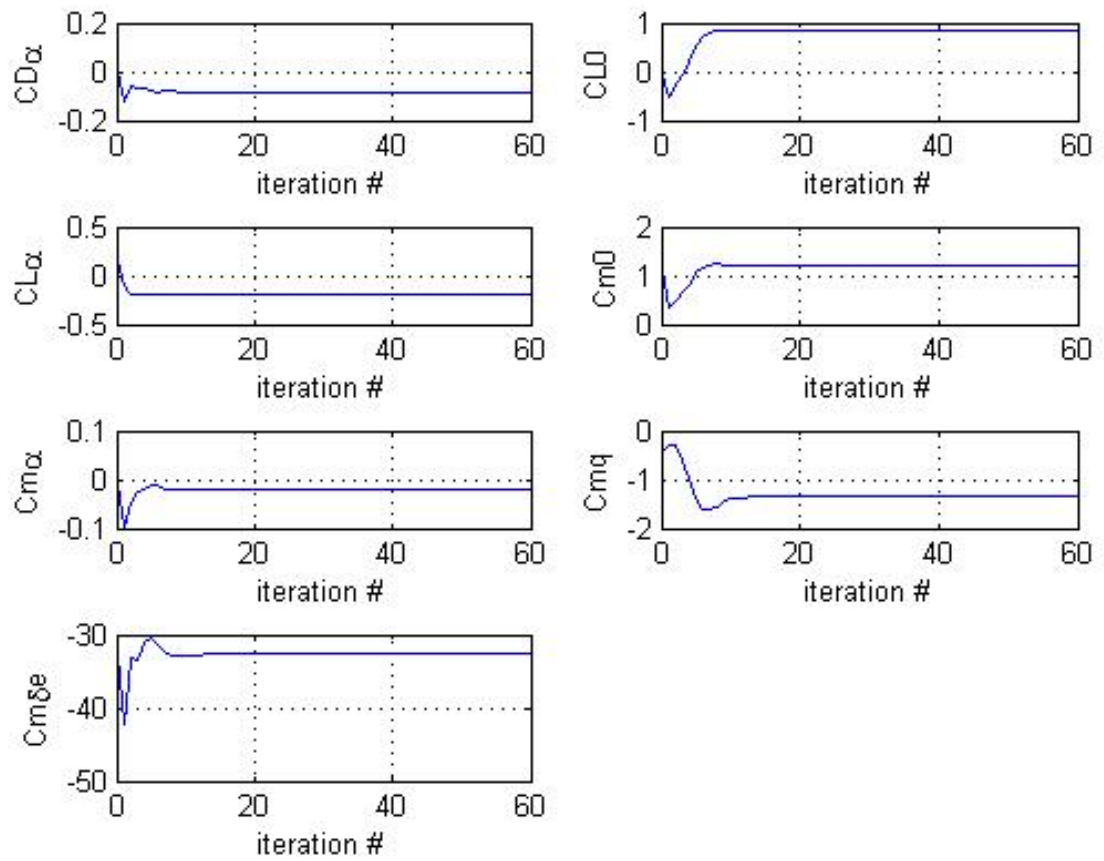


Figure 5.18: Convergence Plots of Non-Dimensional Derivatives for Longitudinal Directional Motion of Aircraft

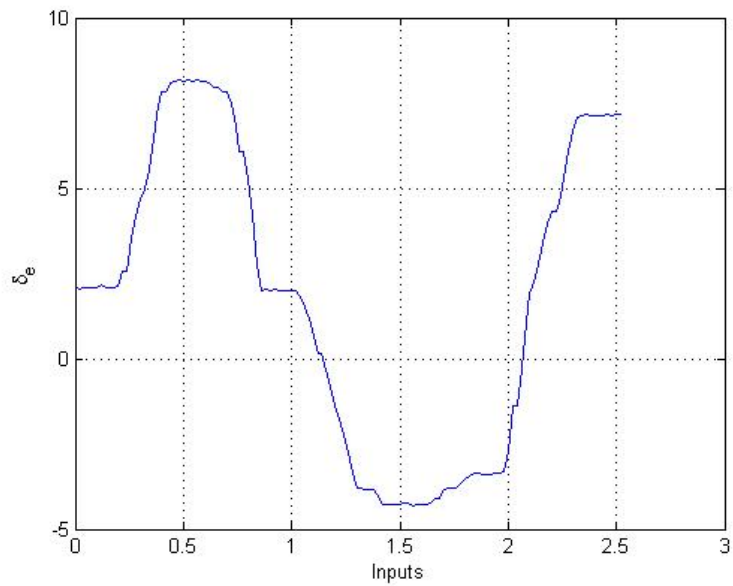


Figure 5.19: Input for Longitudinal Motion

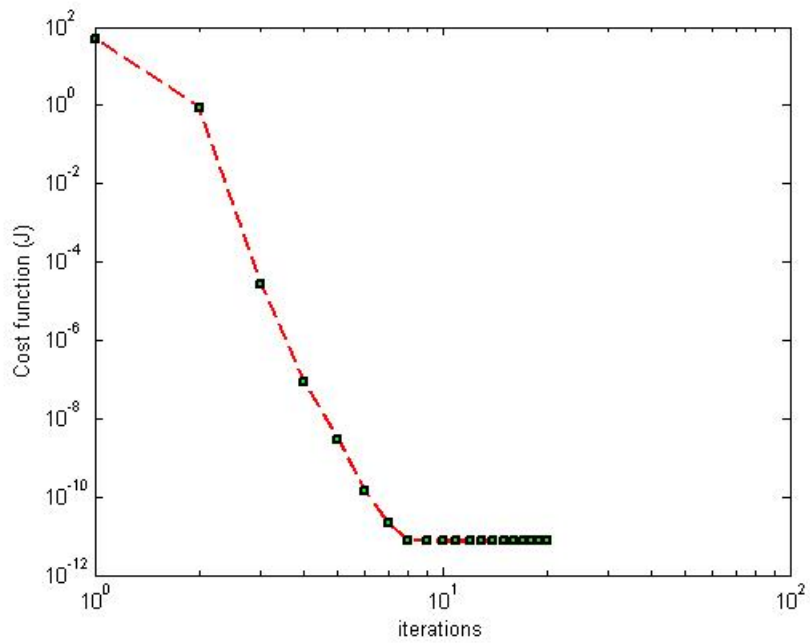


Figure 5.20: Cost Function Reduction for Longitudinal Motion

5.4 Model Validation

Model validation is the final step in the system identification process and must be performed regardless of the accuracy of the parameter estimation techniques. The prime reason for above statement is: estimates are not facts. The identified model must prove that its parameters have physically acceptable values with reasonable accuracy and the best prediction capability. Due to these arguments, the estimated parameters are compared with the available aircraft aerodynamics data, which are obtained from wind tunnel experiments, computational fluid dynamics or theoretical predictions. While comparing these parameters, accuracy and precision of the estimates must be taken in to account. Model validation is very important to gain confidence in the identified model.

CHAPTER 6

SUMMARY

6.1 Concluding Notes

The system identification technique applied to aircraft is an efficient method for aircraft aerodynamic modeling, based on flight test data. This thesis traced several breakthroughs and achievements in the field of system identification, especially application to aircraft. The thesis started with the definition, meaning and significance of system identification and also included the necessity for it. Minimization of the maximum likelihood function was explained in detail.

Presently, this technique involves five fundamental steps: model postulation, experimental design, data analysis, parameter estimation, and model validation. All of them were explained in detail in this thesis. The filter error technique for data analysis was discussed in detail, for both linear and nonlinear dynamical systems. Theoretical techniques for predicting aircraft stability and control derivatives were explained in some details.

The final part of the thesis included successfully investigated examples of system identification using flight test data with results and comparison of the estimated parameters with published data. Using the efficient results derived and presented in this thesis, and also high quality results of many other applications published recently [92-94], a conclusion is be made that many of the application fields which were thought as growing areas few

years before are now more or less, well established. The system identification methods are now highly matured, efficient and sophisticated tools; not only for the research purposes, but also to support and to satisfy the requirements of the aeronautical industry.

6.2 Expected Future Applications of System Identification to Aircraft

There are many interesting and necessary applications of system identification techniques to aircraft which can be studied in the future. Correlation between computational fluid dynamics (CFD) practitioners and system identification researchers should increase considerably. In addition to the use of the system identification technique to validate the wind tunnel and the CFD data, it should also be utilized in coordinated approaches with the CFD, to gain advantages of the strengths of both the techniques or if one approach can not be used efficiently somewhere, another technique can be used to fill in the gaps.

The test data of each individual parts of any aircraft can be measured using small and inexpensive sensors. Using the modern computation capabilities, the aircraft can be identified as distributed parameter models for the aircraft aerodynamics. Effects of each individual sections can be considered as a results of that. This might not be an easy task, as distributed models need more test data of each individual part, improved dynamical models and the best wind tunnel and CFD data. The system identification researchers should then progress towards controlled automated process and solve the particular problems if encountered.

A lot of research work can be done with the nonlinear systems and unsteady aerodynamic models. It includes learning the basic techniques to design related experiments. These should also ensure the necessary and critical experiments are being performed at safe environment and at effective cost; providing the state estimates are accurate and validated models are appropriate. System identification techniques for the nonlinear systems and unsteady aerodynamic modeling are very complex, so the experiments need to be performed with high accuracy and should be repeated.

For few applications, the theoretical and analytical problems will arise in the system identification which can not be ignored. Every new flying vehicle should be tested using the system identification techniques to validate the model. The prime practice, known as the system identification will continue to be an important part in the aeronautical engineering, which involves identification of the mathematical model based on the measured data from the experiment.

BIBLIOGRAPHY

- [1] Jategaonkar, R. V., "Flight Vehicle System Identification: A Time Domain Methodology", edited by Lu, F. K., Vol. 216, Progress in Aeronautics and Astronautics, AIAA, August, 2006, Reston, VA.
- [2] Zadeh, L. A., "From Circuit Theory to System Theory," *Proceedings of the IRE*, Vol. 50, May 1962, pp. 856-865.
- [3] Anon., "He Has a Question for Any Answer," Interview with K. Iliff by M. McCall, Antelope Valley Press, CA, Nov. 1, 1994.
- [4] Jategaonkar, R. V., "Flight Vehicle System Identification - Engineering Utility," *Journal of Aircraft*, Vol. 42, No. 1, 2005, pp. 11.
- [5] Gauss, K. F., "Theory of the Motion of the Heavenly Bodies Moving About the Sun in Conic Section," (Translated by Charles, H. D., 1857), Dover Publications Inc., New York, 1847. (Translated from *Theoria Motus*, 1809)
- [6] Bernoulli, D., "The Most Probable Choice Between Several Discrepant Observations and the Formation Therefrom of the Most Likely Induction," *Acta. Acad. Petrop.*, 1777, pp. 3-33; English Translation by Kendall, M. G., "Daniel Bernoulli on Maximum Likelihood," *Biometrika*, Vol. 48, No. 1, 1961, pp. 1-18.
- [7] Fisher, R. A., "On an Absolute Criterion for Fitting Frequency Curves," *Messenger of Mathematics*, Vol. 41, Macmillan, London, 1912, pp. 155-160.
- [8] Douglas, J., "Theorems in the Inverse Problem in the Calculus of Variations," *Proceedings of the National Academy of Science*, Vol. 16, No. 3, 1940.
- [9] Feldbaum, A. A., "Dual Control Theory," *Automn. Remote Control*, Vol. 22, 1961, pp. 1-12 and 109-121.
- [10] Cuenod, M. and Sage, A., "Comparison of Some Methods Used for Process Identification," *Automatica*, Vol. 4, 1968, pp. 235-269.
- [11] Balakrishnan, A. V. and Peterka, V., "Identification in Automatic Control Systems," *Automatica*, Vol. 5, 1969, pp. 817-829.
- [12] Astrom, K. J. and Eykhoff, P., "System Identification - A Survey," *Automatica*, Vol. 7, No. 2, 1971, pp. 123-162.

- [13] Eykhoff, P., "System Identification, Parameter and State Estimation," John Wiley and Sons, London, 1974.
- [14] Kolmogorov, A. N., "Interpolation und Extrapolation von Stationären Zufälligen Folgen," *Bulletin of the Academy of Sciences of the USSR Series Mathematics*, Vol. 5, 1941, pp. 3-14.
- [15] Wiener, N., "The Extrapolation, Interpolation and Smoothing of Stationary Time Series," OSRD 370, Report to the Services, Research Project DIC-6037, Massachusetts Inst. of Technology, Cambridge, MA, Feb. 1942.
- [16] Kalman, R. E., "A New Approach to Linear Filtering and Prediction Problems," Transactions of the American Society of Mechanical Engineers, Series D, *Journal of Basic Engineering*, Vol. 82, March 1960, pp. 35-45.
- [17] Astrom, K. J., and Bohlin, T., "Numerical Identification of Linear Dynamic Systems from Normal Operating Records," *Proceedings of the 2nd IFAC Symposium on Theory of Self – Adaptive Control Systems* (England, UK), edited by Hammond, P. H., Plenum, New York, 1966, pp. 96-111.
- [18] Bryan, G. H., "Stability in Aviation," Macmillan, London, 1911.
- [19] Hamel, P. G. and Jategaonkar, R. V., "Evolution of Flight Vehicle System Identification," *Journal of Aircraft*, Vol. 33, No. 1, 1996, pp. 9-28.
- [20] Glauert, H., "Analysis of Phugoids Obtained by a Recording Airspeed Indicator," *Aeronautical Research Council R and M 576*, Jan. 1919.
- [21] Norton, F. H., "The Measurement of the Damping in Roll on a JN4h in Flight," NACA Rept. 167, 1923.
- [22] Norton, F. H., "A Study of Longitudinal Dynamic Stability in Flight," NACA Rept. 170, 1923.
- [23] Kroll, N., Radespiel, R., and Rossow, C., "Accurate and Efficient Flow Solvers for 3D Applications on Structured Meshes," VKI Lecture Series 1994-05, Brussels, Belgium, March 1994.
- [24] Slooff, J. W., and Schmidt, W. (eds.), "Computational Aerodynamics Based on the Euler Equations," AG-325, AGARD, Sept. 1994.
- [25] Hamel, P. G., "Determination of Aircraft Dynamic Stability and Control Parameters from Flight Testing," LS-114, AGARD, May 1981 (Paper 10).
- [26] "Parameter Estimation Techniques and Applications in Aircraft Flight Testing," NASA TN-D-7647, 1974.

- [27] “Methods for Aircraft State and Parameter Identification,” AGARD-CP-172, May 1975.
- [28] Breuhaus, W. O., “Summary of Dynamic Stability and Control Flight Research Conducted Utilizing a B-25J Airplane,” Cornell Aeronautical Lab., Buffalo, NY, Rept. TB-405-F-10, May 1948.
- [29] Milliken, W. F. Jr., “Progress in Dynamic Stability and Control Research,” *Journal of the Aeronautical Sciences*, Vol. 14, No. 9, 1947, pp. 493-519.
- [30] Milliken, W. F., Jr., “Dynamic Stability and Control Research,” *Proceedings of the 3rd Anglo – American Aeronautical Conference*, Brighton, England, UK, 1951, pp. 447-524.
- [31] Seamans, R. C. Jr., Blasingame, B. P., and Clementson, G. C., “The Pulse Method for the Determination of Aircraft Dynamic Performance,” *Journal of the Aeronautical Science*, Vol. 17, No. 1, Jan. 1950, pp. 22-38.
- [32] Greenberg, H., “A Survey of Methods for Determining Stability Parameters of an Airplane From Dynamic Flight Measurements,” NACA TN-2340, April 1951.
- [33] Shinbrot, M., “On the Analysis of Linear and Nonlinear Dynamical Systems From Transient-Response Data,” NACA TN-3288, Dec. 1954.
- [34] Howard, J., “The Determination of Lateral Stability and Control Derivatives From Flight Data,” *Canadian Aeronautics Space Journal*, Vol. 13, No. 3, March 1967, pp. 126-134.
- [35] Shinbrot, M., “A Least-Squares Curve Fitting Method with Applications to the Calculation of Stability Coefficients from Transient Response Data,” NACA TN 2341, April 1951.
- [36] Wolowicz, C. H., and Holleman, E. C., “Stability Derivative Determination from Flight Data,” Rept. 224, AGARD, Oct. 1958.
- [37] Mueller, R. K., “The Graphical Solution of Stability Problems,” *Journal of the Aeronautical Sciences*, Vol. 4, No. 8, 1937, pp. 324-331.
- [38] Doetsch, K. H., “The Time Vector Method for Stability Investigations,” *Royal Aircraft Establishment Rept.*, Aero 2495, Aug. 1953.
- [39] Sternfield, L., “A Vector Method Approach to the Dynamic Lateral Stability of Aircraft,” *Journal of the Aeronautical Sciences*, Vol. 21, No. 4, 1954, pp. 251-256.
- [40] Wolowicz, C. H., “Considerations in the Determination of Stability and Control Derivatives and Dynamic Characteristics From Flight Data,” AGARD-AR-549, Pt. 1, 1966.

- [41] Rampy, J. M., and Berry, D. T., "Determination of Stability Derivatives From Flight Test Data by Means of High Speed Repetitive Operation Analog Matching," FTC-TDR-64-8, Edwards, CA, May 1964.
- [42] Taylor, L. W. Jr., and Iliff, K. W., "A Modified Newton-Raphson Method for Determining Stability Derivatives From Flight Data," *Second International Conference on Computing Methods in Optimization Problems*, Academic Press, New York, 1969, pp. 353-364.
- [43] Larson, D. B., and Fleck, J. T., "Identification of Parameters by the Method of Quasilinearization," Cornell Aeronautical Lab., Buffalo, New York, Rept. 164, May 1968.
- [44] Taylor, L. W. Jr., Iliff, K. W., and Powers, B. G., "A Comparison of Newton-Raphson and Other Methods for Determining Stability Derivatives From Flight Data," AIAA Paper, 69-315, March 1969.
- [45] Iliff, K. W., "Aircraft Parameter Estimation" AIAA Dryden Lecture in Research for 1987.
- [46] Hamel, P. G., "Flight Vehicle System Identification Status and Prospects," DFVLR-Mitt. 87-22, Nov. 1987, pp. 51-90.
- [47] Grove, R. D., Bowles, R. L., and Mayhew, S. C., "A Procedure for Estimating Stability and Control Parameters From Flight Test Data by Using Maximum Likelihood Methods Employing a Real-Time Digital System," NASA TN-D-6735, 1972.
- [48] Ross, A. J., and Foster, G. W., "FORTRAN Programs for the Determination of Aerodynamic Derivatives From Transient Longitudinal or Lateral Responses of Aircraft," *Royal Aircraft Establishment*, TR-75090, Sept. 1975.
- [49] Maine, R. E., and Iliff, K. W., "A FORTRAN Program for Determining Aircraft Stability and Control Derivatives From Flight Data," NASA TN-D-7831, 1975.
- [50] Nagy, C. J., "A New Method for Test and Analysis of Dynamic Stability and Control," Air Force Flight Test Center, Edwards, CA, AFFTC-TD-75-4, May 1976.
- [51] Mehra, R. K., "Maximum Likelihood Identification of Aircraft Parameters," *Proceedings of the Eleventh Joint Automatic Control Conference of the American Automatic Control Council*, Paper 18-C, Atlanta, GA, June 1970, pp. 442-444.
- [52] Iliff, K. W., and Maine, R. E., "Practical Aspects of Using a Maximum Likelihood Estimation method to extract stability and control derivatives from flight data," NASA TN D-8209, April 1976, pp. 1-34

- [53] Iliff, K. W., and Maine, R. E., "Further Observations on Maximum Likelihood Estimates of Stability and Control Characteristics Obtained From Flight Data," AIAA Paper 77-1133, Aug. 1977, pp. 100-112.
- [54] Jategaonkar, R. V., and Plaetschke, E., "Maximum Likelihood Estimation of Parameters in Linear Systems with Process and Measurement Noise," DFVLR-FB 87-20, June 1987.
- [55] Maine, R. E., and Iliff, K. W., "User's Manual for MMLE3, a General FORTRAN Program for Maximum Likelihood Parameter Estimation," NASA TP-1563, Nov. 1980.
- [56] Taylor, J. S., Powell, J. D., and Mehra, R. K., "The Use of Smoothing and Other Advanced Techniques for VTOL Aircraft Parameter Identification," Final Rept., Naval Air Systems Command Contract N00019-69-C-0534, Systems Control, Inc., Palo Alto, CA, June 1970.
- [57] Gerlach, O. H., "The Determination of Stability Derivatives and Performance Characteristics From Dynamic Maneuvers," Delft Univ. of Technology, Dept. of Aerospace Engineering, Delft, The Netherlands, Rept. VTH-163, March 1971.
- [58] Jonkers, H. L., "Application of the Kalman Filter to Flight Path Reconstruction From Flight Test Data Including Estimation of Instrumental Bias Error Corrections," Delft Univ. of Technology, Dept. of Aerospace Engineering, Delft, The Netherlands, Rept. VTH-162, Feb. 1976.
- [59] Astrom, K. J., "Control Problems in Papermaking," *Proceedings of the IBM Scientific Computing Symposium on Control Theory and Applications*, IBM Data Processing Division, White Plains, New York, 1966, pp. 135-167.
- [60] Kashyap, R. L., "A New Method of Recursive Estimation in Discrete Linear Systems," *IEEE Transactions on Automatic Control*, Vol. AC-15, No. 1, Feb. 1970, pp. 18-24
- [61] Chen, Robert, T. N., and Eulrich, B. J., "Parameter and Model Identification of Nonlinear Dynamical Systems Using a Suboptimal Fixed-point Smoothing Algorithm," *Proceedings of the Twelfth Joint Automatic Control Conference of the American Automatic Control Council*, Paper 7-E2, Aug. 1971, pp. 731-740.
- [62] Yazawa, K., "Identification of Aircraft Stability and Control Derivatives in the Presence of Turbulence," AIAA Paper 77-1134, Aug. 1977.
- [63] Balakrishnan, A. V., "Stochastic System Identification Techniques," *Stochastic Optimization and Control*, edited by H. F. Karreman, John Wiley and sons, London, 1968.
- [64] Balakrishnan, A. V., "Modelling and Identification Theory: A Flight Control Application," *Theory and Applications of Variable Structure Systems*, edited by R. B. Mohler and A. Ruberti, Academic, New York, 1972.

- [65] Iliff, K. W., "Identification and Stochastic Control with Application to Flight Control in Turbulence," Ph.D. Dissertation, Univ. of California, Los Angeles, CA, May 1973.
- [66] Etkin, B., "Dynamics of Atmospheric Flight," John Wiley and Sons, New York, 1972.
- [67] Maine, R. E., and Iliff, K. W., "Formulation and Implementation of a Practical algorithm for Parameter Estimation with Process and Measurement Noise," *SIAM J. Applied Mathematics*, Dec. 1981, pp. 558-579.
- [68] Jategaonkar, R. V., and Plaetschket, E., "Algorithms for Aircraft Parameter Estimation Accounting for Process and Measurement Noise," *Journal of Aircraft*, Vol. 26, No 4, April 1989, pp. 360-372.
- [69] Iliff, K. W., and Taylor, L. W., "Determination of Stability Derivatives from Flight Data Using a Newton-Raphson Minimization Technique," NASA TN D-6579, March 1972.
- [70] Ortega, J. M., and Rheinboldt, W.C., "Iterative Solution of Nonlinear Equations in Several Variables," Academic Press, New York, 1970.
- [71] Balakrishnan, A. V., "Communication Theory," 1968, McGraw-Hill, NY.
- [72] Mehra, R. K., "Identification of Stochastic Linear Dynamic Systems Using Kalman Filter Representation," *AIAA Journal*, Vol. 9, Jan. 1971, pp. 28-31.
- [73] Gelb, A., "Applied Optimal Estimation," The MIT Press, Cambridge, MA, 1974.
- [74] Grewal, M. S., and Andrews, A. P., "Kalman Filtering Theory and Practice," Prentice Hall, Upper Saddle River, NJ, 1993.
- [75] Vaughan, D. R., "A Non-recursive Algebraic Solution for the Discrete Riccati Equation," *IEEE Transactions on Automatic Control*, Vol. AC-15, Oct. 1970, pp. 597-599.
- [76] Potter, J. E., "Matrix Quadratic Solutions," *SIAM Journal of Applied Mathematics*, Vol. 14, May 1966, pp. 496-501.
- [77] Welch, G., and Bishop, G., "An Introduction to the Kalman Filter," SIGGRAPH, Los Angeles, CA, Aug. 2001.
- [78] Maybeck, P., "Stochastic models, estimation and control," Vol. 1, Academic Press, New York, 1979.
- [79] Roskam, J., "Airplane Design Part VI: Preliminary Calculation of Aerodynamic Thrust and Power Characteristics", Vol. 2, 1990, Roskam Aviation and Engineering Corporation, Ottawa, KS.

- [80] Roskam, J., "Airplane Flight Dynamics and Automatic Flight Controls Part I", Vol. 1, 1995, DARcorporation, Lawrence, KS.
- [81] Roskam, J., "Airplane Flight Dynamics and Automatic Flight Controls Part II", Vol. 1, 1998, DARcorporation, Lawrence, KS.
- [82] Raymer, D. P., "Aircraft Design: A Conceptual Approach", Vol. 3, 1999, AIAA, Reston, VA.
- [83] Nelson, R. C., "Flight Stability and Automatic Control", Vol. 2, 1998, McGraw-Hill, NY.
- [84] Plaetschke, E., Mulder, J. A., and Breeman, J. H., "Results of Beaver Aircraft Parameter Identification," DFVLR-FB 83-10, March 1983.
- [85] McRuer, D., Ashkenas, I., and Graham, D., "Aircraft Dynamics and Automatic Control", Princeton Univ. Press, Princeton, NJ, 1973, pp. 292-295.
- [86] Heffley, R. K., Jewell, W. F., Lehman, J. M., and Van Winkle, R. A., "A Compilation and Analysis of Helicopter Handling Qualities Data, Volume One: Data Compilation," NASA CR-3144, Aug. 1979.
- [87] Chowdhary, G. and Jategaonkar, R. V., "Aerodynamic Parameter Estimation from Flight Data Applying Extended and Unscented Kalman Filter," *AIAA Atmospheric Flight Mechanics Conference and Exhibit*, Keystone, Colorado, Aug. 2006, pp. 6146-6163.
- [88] Jategaonkar, R. V., and Balakrishna, S., "Effects of Flap Position on Longitudinal Parameters of HFB-320," TM SE-8602, NAL Bangalore, India, Feb. 1986 and DFVLR-IB 111-85/15, June 1985.
- [89] Mackie, D. B., "A comparison of Parameter Estimation Results from Flight Test Data Using Linear and Nonlinear Maximum Likelihood Methods," DFVLR-FB 84-06, Dec. 1983.
- [90] Iliff, K. W., "Maximum Likelihood Estimation of Lift and Drag from Dynamic Aircraft Maneuvers," *Journal of Aircraft*, Vol. 14, Dec. 1977, pp. 1175-1181.
- [91] Hobby Outlet, 1700 S.E. Mile Hill Dr., Suite 101, Port Orchard, WA 98366.
- [92] Jategaonkar, R. V., Fischenberg, D., and Gruenhagen, W., "Aerodynamic Modeling and System Identification from Flight Data Recent Applications at DLR," *Journal of Aircraft*, Vol. 41, No. 4, 2004, pp. 681-691.
- [93] Wang, K. C., and Iliff, K. W., "Retrospective and Recent Examples of Aircraft Parameter Identification at NASA Dryden Flight Research Center," *Journal of Aircraft*, Vol. 41, No. 4, 2004, pp. 752-764.

- [94] Morelli, E. A., and Klein, V., "Application of System Identification to Aircraft at NASA Langley Research Center," *Journal of Aircraft*, Vol. 42, No. 1, 2005, pp. 12-25.
- [95] Kuo, B. C., "Automatic Control Systems", Prentice Hall Inc., Englewood Cliffs, NJ, 1962.
- [96] Hildebrand, F. B., "Introduction to Numerical Analysis", McGraw-Hill, New York, 1956, pp. 319-323.

APPENDIX A

DISCRETIZATION OF CONTINUOUS-TIME STATE EQUATION

A.1 Need of Discretization

The state equation utilized in the thesis is given below as [1]:

$$\dot{x}(t) = Ax(t) + Bu(t) + b_x \quad (\text{A.1})$$

This is a continuous time equation. The Kalman filter equations are discrete in nature. Therefore, the state equation given above must be converted from a continuous-time state equation to a discrete-time state equation. In the discrete-time case, it is assumed that the input vector $u(t)$ changes only at the equally spaced sampling instants. The discrete-time state equation will be derived, which yields the exact values at $t = kT$, $k = 0,1,2,3\dots N$

The continuous-time state equation is Eq. A.1. Here, kT and $(k+1)T$ are used instead of k and $(k+1)$ in order to clarify the analysis. The discrete-time representation of Eq. A.1 should be as follows [95]:

$$x_{(k+1)T} = \Theta(t)x_{kT} + \Lambda(t)u_{kT} \quad (\text{A.2})$$

The matrices Θ and Λ depend on the sampling period t . Therefore, if the period is fixed, Θ and Λ are constant matrices.

A.2 Determine Θ and Λ

The general integral solution of Eq. A.1 is [95]:

$$x(t) = e^{At}x(0) + e^{At} \int_0^t e^{-A\tau} Bu(\tau) d\tau \quad (\text{A.3})$$

Therefore

$$x_{(k+1)T} = e^{A(k+1)T}x(0) + e^{A(k+1)T} \int_0^{(k+1)T} e^{-A\tau} Bu(\tau) d\tau \quad (\text{A.4})$$

and

$$x_{kT} = e^{AkT}x(0) + e^{AkT} \int_0^{kT} e^{-A\tau} Bu(\tau) d\tau \quad (\text{A.5})$$

If Eq. A.5 is multiplied by e^{AT} and subtracted from Eq. A.4, the following result will be obtained [95].

$$x_{(k+1)T} = e^{AT}x_{kT} + e^{A(k+1)T} \int_{kT}^{(k+1)T} e^{-A\tau} Bu(\tau) d\tau \quad (\text{A.6})$$

That can be simplified to [95]:

$$x_{(k+1)T} = e^{AT}x_{kT} + \int_0^T e^{A\tau} Bu(\tau) d\tau \quad (\text{A.7})$$

Comparing Eq. A.2 and Eq. A.7 [95].

$$\Theta = e^{AT} \quad \text{and} \quad \Lambda = \int_0^T e^{A\tau} d\tau \quad (\text{A.8})$$

Θ is termed the state transition matrix, and Λ is the integral of the state transition matrix.

$$\begin{aligned}\Theta &= e^{AT} \\ \Lambda &= A^{-1}(e^{AT} - I)\end{aligned}\tag{A.9}$$

where I is an identity matrix.

The final discrete-time state equation is given below:

$$\tilde{x}(t_{k+1}) = \Theta \hat{x}(t_k) + \Lambda B \bar{u}(t_k) + \Lambda b_x\tag{A.10}$$

APPENDIX B

NUMERICAL INTEGRATION USING RUNGE-KUTTA METHOD, ORDER 4

A Runge-Kutta algorithm was utilized in this thesis to integrate non-linear equations numerically. Runge-Kutta algorithms use trial steps at the midpoint of each integration interval to cancel out lower order error terms. The fourth-order formula is sometimes known as *RK44*. This method is reasonably simple, robust and also a good general candidate for numerical solution of differential equations when combined with an intelligent adaptive step-size routine [96]. Runge-Kutta Method of order 4 used here assumes the function to be used is continuous-time. The Runge-Kutta method uses following formulae [96]

$$\begin{aligned}t_{k+1} &= t_k + \Delta t \\x_{j+1} &= x_j + \frac{\Delta t}{6}(k_1 + 2k_2 + 2k_3 + k_4)\end{aligned}\tag{B.1}$$

Where k_1, k_2, k_3, k_4 are calculated as [96]:

$$\begin{aligned}k_1 &= k(x, u, \beta) \\k_2 &= k(x + k_1(\Delta t/2), \bar{u}, \beta) \\k_3 &= k(x + k_1(\Delta t/2), \bar{u}, \beta) \\k_4 &= k(x + k_3\Delta t, \bar{u}, \beta)\end{aligned}\tag{B.2}$$